

Toxicogenomics profiling of bone marrow from rats treated with topotecan in combination with oxaliplatin: a mechanistic strategy to inform combination toxicity

Myrtle Davis, Jianying Li, Elaine Knight, Kellye K Daniels and Pierre R. Bushel

Journal Name:	Frontiers in Genetics
ISSN:	1664-8021
Article type:	Original Research Article
Received on:	16 Oct 2014
Accepted on:	12 Jan 2015
Provisional PDF published on:	12 Jan 2015
Frontiers website link:	www.frontiersin.org
Citation:	Davis M, Li J, Knight E, Daniels KK and Bushel PR(2015) Toxicogenomics profiling of bone marrow from rats treated with topotecan in combination with oxaliplatin: a mechanistic strategy to inform combination toxicity. <i>Front. Genet.</i> 6:14. doi:10.3389/fgene.2015.00014
Copyright statement:	© 2015 Davis, Li, Knight, Daniels and Bushel. This is an open-access article distributed under the terms of the Creative Commons Attribution License (CC BY) . The use, distribution and reproduction in other forums is permitted, provided the original author(s) or licensor are credited and that the original publication in this journal is cited, in accordance with accepted academic practice. No use, distribution or reproduction is permitted which does not comply with these terms.

This Provisional PDF corresponds to the article as it appeared upon acceptance, after rigorous peer-review. Fully formatted PDF and full text (HTML) versions will be made available soon.

Toxicogenomics profiling of bone marrow from rats treated with topotecan in combination with oxaliplatin: a mechanistic strategy to inform combination toxicity

Myrtle Davis^{1,*}, Jianying Li^{2,4}, Elaine Knight¹, Sandy R. Eldridge¹, Kellye K. Daniels³ and Pierre R. Bushel^{4,5,*}

¹ National Cancer Institute, Toxicology and Pharmacology Branch, Division of Cancer Treatment and Diagnosis, Bethesda, MD 20892, USA

² Kelly Government Solutions, Research Triangle Park, NC 27709, USA

³ Southern Research Institute, Toxicology and Pathology Services, Birmingham, AL 35205, USA

⁴ National Institute of Environmental Health Sciences, Microarray and Genome Informatics Group, Research Triangle Park, NC 27709, USA

⁵ National Institute of Environmental Health Sciences, Biostatistics Branch, Division of Intramural Research, Research Triangle Park, NC 27709, USA

***Corresponding Authors**

Toxicology and Toxicogenomics:

Dr. Myrtle Davis

9609 Medical Center Drive

Bethesda, MD 20892

Phone: 240-276-5915

myrtledavis@mail.nih.gov

Bioinformatics and Toxicogenomics:

Dr. Pierre R. Bushel

111 T.W. Alexander Drive

Research Triangle Park, NC 27709

Phone: 919-316-4564

bushel@niehs.nih.gov

Running Title: Toxicogenomics profiling of bone marrow

Keywords: Toxicogenomics, Bone Marrow, Topotecan, Combination, Oxaliplatin, Enhanced Toxicity, EPIG

Word Count (excluding references): 6,663

Total number of figures and tables: 11

Abstract

Combinations of anticancer agents may have synergistic anti-tumor effects, but enhanced hematological toxicity often limit their clinical use. We examined whether “microarray profiles” could be used to compare early molecular responses following a single dose of agents administered individually with that of the agents administered in a combination. We compared the mRNA responses within bone marrow of Sprague-Dawley rats after a single 30-minute treatment with topotecan at 4.7 mg/kg or oxaliplatin at 15 mg/kg alone to that of sequentially administered combination therapy or vehicle control for 1, 6 and 24 hours. We also examined the histopathology of the bone marrow following all treatments. Drug-related histopathological lesions were limited to bone marrow hypocellularity for animals dosed with either agent alone or in combination. Lesions had an earlier onset and higher incidence for animals given topotecan alone or in combination with oxaliplatin. Severity increased from mild to moderate when topotecan was administered prior to oxaliplatin compared with administering oxaliplatin first. Notably, six patterns of co-expressed genes were detected at the 1-hour time point that indicate regulatory expression of genes that are dependent on the order of the administration. These results suggest alterations in histone biology, chromatin remodeling, DNA repair, bone regeneration, and respiratory and oxidative phosphorylation are among the prominent pathways modulated in bone marrow from animals treated with an oxaliplatin/topotecan combination. These data also demonstrate the potential for early mRNA patterns derived from target organs of toxicity to inform toxicological risk and molecular mechanisms for agents given in combination.

1 Introduction

2
3 Effective anticancer treatments generally require the use of a combination of drugs. A challenge for
4 combination treatment is a shift in the extent and severity of adverse effects for the combination compared
5 with either of the agents when given alone. Most Phase I trials for targeted agent combinations have been
6 designed to escalate the drug doses to the maximally tolerated dose (MTD). Data that are now available
7 suggest that combinations of molecularly targeted agents (MTAs) can lead to more severe toxicities and that
8 dose reduction is often required for regimens to be tolerable (Kummar et al., 2010). Although empirical
9 approaches are currently being used, a preclinical assessment that can provide a mechanistic basis for
10 adverse effects of drug combinations is desirable. Systems-based computational approaches that integrate,
11 transcriptomics, proteomics, or other profiling data may be useful to discover network-level alterations in
12 normal cell signaling in normal tissues after *in vivo* administration.
13

14 Toxicogenomics, the application of transcription profiling to toxicology (Nuwaysir et al., 1999), has been
15 widely used for elucidating the molecular and cellular actions of drugs and chemicals on biological systems,
16 flagging potential for toxicity before functional damages occur, and providing classification of known or
17 new toxicants based on signatures of gene expression (Guerreiro et al., 2003; Ruepp et al., 2005; Bushel et
18 al., 2007; Chengalvala et al., 2007; Ganter et al., 2008; Ryan et al., 2008). In the current study, we examined
19 the benefit of applying transcriptomics for risk assessment of enhanced target organ toxicity when two
20 drugs are used in combination. We hypothesized that an additive toxicity pattern can be inferred from
21 comparative analysis of early mRNA responses of tissues obtained following a single dose of two agents
22 given individually or in combination and additive toxicity is expected. We also anticipate that biological
23 pathways revealed by gene response patterns will provide a more comprehensive understanding of toxicity
24 and provide a mechanistic basis to trigger experimental investigation.
25

26 For this initial proof of concept, we used the chemotherapeutic agents topotecan and oxaliplatin, the two of
27 which have been explored for use in combination for treating various cancers (Alexandre et al.,
28 2002; Tortora et al., 2002; Elkas et al., 2007). Topotecan is a topoisomerase I (topo I) inhibitor that forms a
29 complex on DNA leading to double-stranded DNA breaks and ultimately cell death. Oxaliplatin is a
30 diaminocyclohexane platinum compound that acts as a DNA alkylating agent. Pre-exposure to oxaliplatin
31 transiently increased Topo I-mediated single-strand breaks, suggesting that DNA platination might stimulate
32 Topo I DNA cleavage activity providing a rationale for the use of platinum-based compounds with
33 topoisomerase inhibitors (Goldwasser et al., 1999). Combinations of topo I inhibitors and platinum
34 derivatives, in general, have synergistic anti-tumoral effects, but their clinical use is limited by
35 hematological toxicity, which is clearly dependent on the sequence of drug administration. We also wanted
36 to examine the possibility that the acute response of a target organ to a single dose of treatment and
37 obtaining an associated molecular footprint can aid in investigation about mechanisms of target-mediated
38 toxicity. In our study, a single dose of topotecan was given to Sprague Dawley rats either before or after
39 administration of oxaliplatin to determine whether combination administration or the order of administration
40 affected the bone marrow toxicity and the microarray signature profile obtained following combined
41 administration of the drugs. We found that a single dose intravenous infusion of topotecan or oxaliplatin,
42 given alone or in combination, to male rats resulted in the formation of histopathological lesions in bone
43 marrow (hypocellularity) observed after only 1 hour of topotecan administration or 6 hours after oxaliplatin
44 administration. The severity of bone marrow lesions increased when topotecan was given prior to
45 oxaliplatin compared with oxaliplatin given prior to topotecan indicating that severity of toxicity was
46 affected by sequence of administration.
47

48 We also characterized the molecular and pathway signatures in bone marrow for a topotecan/oxaliplatin
49 combination based on global gene expression analyses and comprehensive bioinformatics profiling. We

examined the bone marrow tissue for histopathological lesions. Based on our results, we propose that single dose rodent studies and microarray analysis of mRNA patterns derived from affected tissues represents a mechanistic approach to evaluate the potential risk of enhanced toxicity for combination agents.

Materials and Methods

Test Articles

Oxaliplatin (1.2 g; NSC 266046) and topotecan (310 mg; NSC 609699) were supplied by the National Cancer Institute (NCI) and received at Southern Research Institute on October 19, 2010. The test articles were received on dry ice and then refrigerated. The following reagents were received from the NCI chemical repository and stored at room temperature and used in the preparation of dose formulations: 5% dextrose injection, USP (PSS World Medical; Kennesaw, GA); Saline Solution 0.9% (saline; Nova Tech Inc.; Grand Island, NE).

Dose Formulation Preparation

Dose formulations of topotecan were prepared in saline to contain a nominal concentration of topotecan hydrochloride of 1.2 mg/mL. For preparation, the appropriate amount of saline was added to the required amount of topotecan hydrochloride and the formulation was stirred until a solution was obtained. Dose formulations of oxaliplatin were prepared in 5% dextrose in water (D5W) to contain a nominal concentration of oxaliplatin of 3.75 mg/mL. For preparation, the appropriate amount of D5W was added to the required amount of oxaliplatin and the formulation was stirred until a solution was obtained.

Animals and Treatments

The 96 Sprague-Dawley male rats used in this study were obtained from Charles River Laboratories, Inc. (Raleigh, NC). Each rat was procured with an indwelling femoral vein cannula. Animals were given a unique identification number by ear punch. Prior to dosing on day 1, the catheter of each rat was checked for patency. Rats with patent catheters were randomly assigned to one of 8 treatment groups. On day 1, the rats were approximately 8 weeks of age and weighed between 271.2 to 342.2 g. Teklad Certified Rodent Diet 2016C (Harlan; Madison, WI) and tap water (Birmingham public water supply) were provided ad libitum to the rats prior to and throughout the study. The animals were individually housed in solid-bottom polycarbonate cages on stainless steel racks in a room maintained at a temperature of 70-79°F and a relative humidity of 44-66%. Room lights were controlled by an automatic timer set to provide a 12/12 light:dark cycle. Heat-treated hardwood chip bedding (P.J. Murphy Forest Products, Corp.; Montville, NJ) was used as bedding material. No known contaminants were present in the food, water, or bedding that would be expected to interfere with or affect the outcome of the study. Cage size and animal care conformed to the guidelines of the Guide for the Care and Use of Laboratory Animals (Bakheet, 2011) and the U.S. Department of Agriculture through the Animal Welfare Act (Public Law 99-198).

The study design with doses administered is provided in Table 1. A dose slightly below the MTD was chosen for these studies. Since the goal of our study was to investigate gene responses induced by a single dose that could potentially be premonitory for toxicity, we administered a dose that would not be confounded by marked pathological changes in the tissue. The MTD for oxaliplatin in rats was referenced in the Center for Drug Evaluation and Research pharmacology review of NDA # 21-492 (via NDA 21-063 (FDA, 2002)) for oxaliplatin and is close to the human clinical dose of 85 mg/m². The dose selected for topotecan was derived from the time course of the hematological effects of topotecan after two consecutive daily administrations to tumor-bearing rats that was described using a semiphysiological model to predict

the hematotoxic effects of topotecan (Friberg et al., 2002; Segura et al., 2004). Each rat was administered a single intravenous (IV) infusion dose, given over a 30-minute interval, of topotecan (of 4.7 mg/kg), oxaliplatin (15 mg/kg), or respective vehicle control formulation, see Table 1. Thirty minutes after the end of the first infusion, topotecan, oxaliplatin, or a respective vehicle control formulation was administered by IV infusion, given over a 30-minute interval. For example, animals given topotecan (or corresponding vehicle) during the first infusion were given oxaliplatin (or corresponding vehicle) during the second infusion. All doses were delivered at a flow rate of approximately 4 mL/kg/30 minutes. Infusion volumes were based on the mean body weight of animals on the day prior to dosing. Rats were observed twice daily during the pre-study and study periods for signs of mortality and morbidity. Detailed clinical examinations of each rat were collected prior to euthanasia. Each animal was weighed on the day of dosing prior to dose administration (for the calculation of infusion rate; data not reported).

Histopathology

Samples of femur bone marrow were collected for histopathology and fixed in 10% neutral buffered formalin. All slides were examined by a veterinary pathologist. Each lesion was listed and coded by the most specific topographic and morphologic diagnoses, severity, and distribution using Toxicology Data Management System (TDMS) nomenclature. A four-step grading system was used to rank the severity of microscopic lesions for comparison among groups.

Tissue Collection and RNA Isolation

At 1, 6, or 24 hours after the completion of dosing, 4 rats per group were euthanized by CO₂ asphyxiation. Immediately after euthanasia, bone marrow from left femurs was collected for RNA isolation. Bone marrow was flushed from bone using RNeasy[®] and refrigerated (approximately 2-8°C) for at least 24 hours and then stored at or below -20°C.

RNA isolation from individual tissues was accomplished using an RNeasy microarray kit (QIAGEN Inc., Valencia, CA). After extraction, the RNA concentration of each sample was determined using a RiboGreen assay. The RNA Integrity Number (RIN) of each sample was determined using an Agilent 2100 Bioanalyzer with 2100 Expert Software (Version B.02.06.S1418; Agilent, Santa Clara, CA). Only samples with a RIN of 7.5 or higher were deemed acceptable for gene expression analysis. Two samples, a group 3 and one from group 2 did not meet the RIN for further processing. Each of the remaining RNA samples were diluted to the required concentration (250 ng/μL) and then stored at or below -70°C prior to shipment to Expression Analysis (Durham, NC) for microarray hybridization.

Microarray Hybridization

Microarray data was generated by Expression Analysis (Durham, NC). RNA samples were converted into labeled target antisense RNA (cRNA) using the Single-Round RNA Amplification and Biotin Labeling System (Enzo Life Sciences, Farmingdale, NY). Briefly, 2.5 μg of total RNA was converted into double stranded cDNA via reverse transcription using an oligo-d(T) primer-adaptor. This cDNA was purified and used as a template for *in vitro* transcription using T7 RNA polymerase and biotinylated ribonucleotides. The resulting cRNA was purified using magnetic beads and quantitated using spectrophotometry. Next, 11 μg of purified cRNA was fragmented using a 5X fragmentation buffer (200 mM Tris-Acetate, pH 8.1, 500 mM KOAc, 150 mM MgOAc), then a hybridization cocktail was prepared and added to the fragmentation product using the Hybridization, Wash and Stain kit (Affymetrix, Santa Clara, CA), applied to Affymetrix GeneChip Rat Genome 230 2.0 Arrays, and incubated at 45°C for 16 hours. Following hybridization,

arrays were washed and stained using standard Affymetrix procedures before scanning on the Affymetrix GeneChip Scanner 3000 using factory PMT settings. Data extraction was completed with Expression Console software using a target scaling of 500. The data are available in the Chemical Effects in Biological Systems (CEBS) repository (Waters et al., 2008) under investigation accession number: 007-00005-0000-000-2 and study accession number: 007-00005-0001-000-3 as well as in the Gene Expression Omnibus (GEO) (Edgar et al., 2002;Barrett et al., 2013) under accession number GSE63902.

Detection of Differentially Expressed Genes (DEGs)

Data analysis was performed using the Bioconductor R package (Gentleman, 2005). We used the package "affyQCReport", combined with principal component analysis (PCA), for array quality control (i.e. outliers detection). After the one outlier sample was excluded (sample 1344-05H, 6 hours oxaliplatin followed by vehicle), the remaining Affymetrix raw CEL files were preprocessed using the robust multichip average (RMA) algorithm (Irizarry et al., 2003a); which includes background correction, quantile normalization, and summarization by the median polish approach. Next, we performed PCA-based gene filtering on the \log_2 scale data from RMA using the package "pvac", where the filtering is based on a score measuring consistency among probes within a probe set (Irizarry et al., 2003b). Finally, the statistical significance of DEGs was accessed by comparison of treated samples to time-matched controls using the empirical Bayes based method known as a limma t-test, which is available in the bioconductor package LIMMA (Smyth, 2005). Analyses were carried out in two batches, where the first batch includes samples from groups 1, 3, 5 and 7, and the second batch contains samples from groups 2, 4, 6, and 8, (see study design Table 1).

Detection of Patterns of Co-Expressed Genes

\log_2 scaled data of the probes remaining after the PCA-based filtering were analyzed for expression patterns across the samples using methodology known as extracting gene expression patterns and identifying co-expressed genes (EPIG) (Chou et al., 2007). For each treatment group, the pixel intensity data for each probe was converted to a ratio value by dividing the average probe pixel intensity by the 1-hour control samples from that group and then taking the log base 2. EPIG uses correlations (r) across all the sample groups, signal to noise ratio (s/n) within groups of samples, and magnitude of fold change (FC) for a probe within a group to first detect all potential patterns in the data, and then categorize each probe to the pattern that is most statistically significant in terms of the correlation between the probe profile and the pattern. The parameter settings for the EPIG analysis were the defaults: $r = 0.8$, $s/n = 2.5$ and $FC = 0.5$. We used a minimum pattern cluster size of 6 for finding all potential patterns.

Enrichment of Biological Processes Based on DEGs

For each DEGs list derived at p -value < 0.01 and absolute fold change > 2 , the Affymetrix GeneChip Rat Genome 230 2.0 Array probe sets were mapped to the Gene Ontology (GO) biological processes (BPs) of the genes they represent using version 2.10.1 of the GO database and the rat2302 database. The 2.14.0 version of the topGO Bioconductor package in R was used to perform enrichment of GO BP terms. The classic algorithm (where the significance of a node is considered independent of the significance of the neighboring nodes) and Kolmogorov-Smirnov test statistic were used for enrichment with node size of at least 5 DEGs. Significance of enrichment was set to p -value < 0.05 . The union of the enriched GO BPs terms from all of the DEGs lists yielded 641 terms. BP terms which were not significant had missing p -values and were imputed with 1.0. The 641 GO BPs terms were clustered based on the $-\log_{10} p$ -values and using Pearson correlation (r) as the dissimilarity metric with average linkage grouping. Clusters (those with a $1 - r$ value ≥ 0.9) of GO BP terms ($n \geq 30$) were labeled according to the node having the maximum number of paths to it within the GO BP subtree directed acyclic graph derived from the terms in the cluster.

Pathway Analysis of Genes within Patterns Extracted by EPIG

Clusters of genes identified by EPIG were analyzed using Pathway Studio 9[®] (Ariadne Genomics, Rockville, MD), to find enriched pathways. Enrichment analysis in Pathway Studio 9[®] was performed by Gene Set Enrichment Analysis (GSEA) and Sub-Network Enrichment Analysis (SNEA) algorithms. Functional enrichment was performed using Fisher's exact test. SNEA enrichment in Pathway Studio was calculated using the Mann-Whitney test, a nonparametric method for comparing the medians of two distributions. Significant enrichment was set at p-value < 0.05. For GSEA, pathways with fewer than 3 entities represented were filtered from the data sets.

Visualization of Gene Expression on Pathways

To visualize the changes of gene expression within a particular pathway, Pathvisio version 3.1.3 (van Iersel et al., 2008) was used to overlay the average of the log base 2 ratio values from the replicate samples onto biological pathways obtained from Wikipathways (Kelder et al., 2012). The cluster IDs from UniGene (according to the rat Rn4 July 12, 2012 release of refSeq version 54) was used to map the probe sets on the microarray to the genes on the Wikipathways.

Gene Regulatory Network Reconstruction

The Gene Regulatory Network Inference (GRNInfer) software (Wang et al., 2006) with default parameter settings ($\lambda = 0.0$ and threshold = 1×10^{-6} controlling the sparseness and the complexity of the network respectively) was used to reconstruct the interactions of the 19 genes in the p53 signaling Wikipathway that had gene expression data mapped. The gene expression data from microarray probes mapping to the same UniGene cluster were averaged and then biological replicates at each time point were averaged. GRNInfer uses linear programming and singular value decomposition of the time point gene expression data to derive of the interactions of the genes within the network given the above thresholds. For topotecan followed by oxaliplatin and oxaliplatin followed by topotecan, the averaged gene expression measures at each time point were used to reconstruct the gene regulatory network depending of the order of administration of the two drugs.

Results

Clinical Observations

No mortality occurred during the study and no drug- or treatment-related adverse clinical signs were observed for any animal during the study. The mean body weight of animals in the individual dose groups ranged from 300 to 310 g on the day of dosing.

Histopathology

Bone marrow hypocellularity was observed in the bone marrow of animals dosed with topotecan, oxaliplatin, or a combination of these two drugs (Figure 1 and Table 2). Minimal bone marrow hypocellularity consisted of an approximately 10 to 20% decrease in the normal population of cells which reside in the bone marrow in comparison with control animals. The remaining cell population consisted primarily of band and mature granulocytes (neutrophils and eosinophils), mature erythrocytes, and megakaryocytes. Occasionally apoptotic cells were observed in the bone marrow of some animals. These lesions were observed as early as 1 hour after the end of topotecan administration and 6 hours after the end of oxaliplatin administration. Bone marrow hypocellularity was observed at a higher and earlier onset of incidence in animals that received topotecan alone or topotecan in combination with oxaliplatin than in dose groups that received only oxaliplatin. One-hour post treatment, bone marrow hypocellularity was observed for animals in all of the dose groups administered topotecan alone or topotecan in combination with oxaliplatin, but not in the dose groups given only oxaliplatin. There also appeared to be an increase in severity of bone marrow suppression from mild to moderate when topotecan was given prior to oxaliplatin

than when oxaliplatin was given prior to topotecan. These data support a sequence dependency for the severity of bone marrow toxicity for this combination.

RNA Isolation

The integrity of each isolated RNA sample was equal to or greater than the protocol-specified minimum RIN (7.5), with the exception of two samples. Acceptance criteria could not be obtained for bone marrow collected from one of the animals from group 3 (topotecan/D5W treated group) and one animal in group 2 (D5W/saline vehicle control group). These samples were not submitted for gene expression analysis.

Patterns of Co-expressed Genes

We focused our analysis on uncovering groups of genes displaying similarity in their expression patterns and comparing the gene responses between treatment groups. The EPIG approach utilizes the underlying structure of gene expression data to extract patterns and identify co-expressed genes that are responsive to experimental conditions (Chou et al., 2007). The response patterns of genes were used to select gene sets that represent potential signatures for effects of the combination treatments that differed from that of the single agents. As shown in Figures 2A, 2B, and 2C, several patterns of gene expression are induced or repressed relative to time-matched controls at the 1-hour, 6-hour or 24-hour time points respectively. Patterns that identified differences between individual treatment and combination treatment groups are marked with an asterisk in Supplementary Figures 1A, 1B and 1C. The Venn diagrams in Supplementary Figure 2 reveal that there is little overlap of co-expressed genes changes (of 4 fold or more) between oxaliplatin and topotecan except for at the 24-hour time point where 73 genes overlap.

The heat map in Figure 3A shows gene expression patterns across all treatment groups and time points. There is a clear time response in the patterns of gene expression from the treatments where by the 24-hour time point, the patterns of expression are either maximally induced or maximally repressed. A list of representative pattern-specific genes showing at least 4-fold differences from their respective controls at the 24-hour bone marrow collection time point is provided in Table 3 (up-regulated) and Table 4 (down-regulated). Notably, several genes related to chondrogenesis, bone repair, and differentiation were profoundly increased in response to combination treatment when compared to individual treatments. As show in the visualization of just the 1-hour time points (Figure 3B), the co-expressed genes in patterns 8 & 9 and pattern 11 vary depending on whether topotecan was given before or after the vehicle or oxaliplatin. On other hand, the co-expressed genes in patterns 14 – 16, vary depending on whether oxaliplatin was given before or after the vehicle. The 244 probes in patterns 8, 9 and 11, representing 59 co-expressed genes, enrich for pathways related to mRNA splicing, spliceosomes, metabolism, cell cycle and DNA replication. The 188 probes in patterns 14 – 16, representing 45 co-expressed genes, enrich for pathways related to chromosome organization, chromatin packaging and remodeling. Full lists of genes derived from each pattern with absolute fold change of 4 or greater from their respective controls and $p < 0.05$, are provided in Supplementary Table 1.

Pathway Analysis of Genes within Patterns Extracted by EPIG

Gene lists within patterns revealing clear differences between control and treatment groups for each time-point were used to obtain pathway enrichment profiles by gene set enrichment analysis (Subramanian et al., 2005). Supplementary Tables 2, 3 and 4 are lists of pathways from gene set enrichment analyses carried out against reference pathways, provided by Ariadne, within the designated patterns. Pathways common to multiple patterns were also identified and shown in Figure 4. The pathways commonly enriched in all patterns evaluated at all treatment times were those pathways related to chromatin remodeling and cell cycle regulation. Pathways derived from the lists of genes obtained from bone marrow samples 1 and 6 hours after dosing were particularly enriched with pathways related to DNA repair, histone biology, cell cycle regulation, hypoxia, glutathione metabolism, and respiratory and oxidative phosphorylation. These

293 regulatory events provide evidence of target-mediated biology for the drug treatments that can be potentially
294 used as a basis for additional toxicodynamic modeling as early as 1 hour after administration of a single
295 dose.

296 297 *Differentially Expressed Genes*

298 Using statistical comparisons of treatments to time-matched controls (absolute fold change > 2 and FDR <
299 0.01), 3304 gene probes in total were detected as differentially expressed (Supplementary Table 5).
300 Principal component (PC) analysis of the gene expression data from the differentially expressed gene probes
301 projected the samples in 3-dimensional space (Supplementary Figure 3) and revealed that PC #1 separates
302 the samples by time and the top 3 PCs grouped the biological replicates by treatment very well.

303 304 *Enrichment of Biological Processes*

305 Genes detected as differentially expressed at each time point (Supplementary Table 5) were used to enrich
306 Gene Ontology (GO) biological processes (BPs). There were 641 GO BPs (Supplementary Table 6)
307 significant (p -value < 0.05) from the union of all the lists (Supplementary Tables 7-12). Figure 5 shows the
308 clustering of the 641 GO BPs terms based on the $-\log$ base 10 p -values. Clusters (those with a correlation
309 value ≥ 0.9) of GO BP terms ($n \geq 30$) were labeled according to the node having the maximum number of
310 paths to it within the GO BP subtree directed acyclic graph derived from the terms in the cluster. DNA
311 damage-signal transduction by p53 was highly enriched by the oxaliplatin exposure at the 6-hour time point
312 when it was given first but not second. Oxaliplatin given second elicited an ATP catabolic process at 6-
313 hours and positive regulation of epithelial to mesenchymal transition at 24-hours. Topotecan when given
314 second at 6-hours impacted Ras GTPase activity in a positive regulation manner. The GTP catabolic process
315 was enriched at the 6-hour time point regardless of the order of administration of topotecan or oxaliplatin.
316 Very few BPs were enriched at the 1-hour time points. However, the biological processes highly connected
317 to ventricular cardiac muscle cell development were enriched in a time-dependent manner, maximizing at
318 the 24-hour time point.

319 320 321 *Regulation of p53 Signaling, Apoptosis and Cell Cycle Related Genes*

322 Pathways related to DNA damage and p53-mediated cell cycle arrest were identified as highly connected
323 and were uniquely enriched in some samples. We then visualized the changes in gene expression within the
324 rat p53 signaling Wikipathway at the 24-hour time point in the study (Figure 6). As indicated by the
325 relative expression to time-matched controls, MDM2, GADD45, SCOTIN, CASP8 and IGFB3 were up-
326 regulated whereas the cyclins, p53, SIAH, GTSE1 and PARP1 were down-regulated. Regulation of several
327 genes that also play roles in the apoptosis pathways (Figure 4) and cell cycle regulation (Figure 4) was also
328 observed at the 24-hour time point.

329 330 331 *p53 Signaling Pathway Gene Regulatory Network Reconstruction*

332 The enrichment of GO biological processes from the samples where oxaliplatin is given first followed by
333 vehicle for topotecan revealed DNA damage, regulation of p53 signaling transduction (Figure 5). In
334 addition, the overlay of gene expression data on the p53 signaling pathway revealed regulation of key
335 components of the cascade at 24-hours (Figure 6). We therefore sort out to reconstruct the gene regulatory
336 network based on the 19 genes mapped to the rat p53 signaling Wikipathway. This would allow us to
337 compare the gene interactions from the time point data in the samples where topotecan is given first
338 followed by oxaliplatin vs when oxaliplatin is given first followed by topotecan. Using the Gene
339 Regulatory Network Inference (GRNInfer) software with the default setting to control the sparseness and
340 the complexity of the network reconstruction, gene networks based on the average of the four replicate time
341 point studies for each order of administration were revealed (Figure 7). When topotecan is given first

followed by oxaliplatin, MDM2 proto-oncogene, E3 ubiquitin protein ligase (MDM2) and GADD45g are central hubs interacting with p53, cyclin-dependent kinases, several cysteine-aspartic acid proteases (CASP8 and CASP3) and other components (Figure 7A). On the other hand, when oxaliplatin is given first followed by topotecan, CASP8 and the G-2 and S-phase expressed 1 gene (GTSE1) are the central hubs of the network interacting with p53, the cyclin-dependent kinases, CASP9, Kras, FAS, BID and other components (Figure 7B). Essentially the activation and inactivation shown for components in the networks are caused by different central regulators depending on the order of administration.

Discussion

This study was conducted to determine whether a single dose rodent study and toxicogenomics profiling informs the potential risk for enhanced bone marrow toxicity for the combined administration of clinically effective chemotherapeutic agents. Genomic profiling is a mature technology that has been strategically and efficiently used in preclinical drug safety assessment to predict safety issues that may be revealed in more lengthy, longer-term studies (Ryan et al., 2008;Huang et al., 2010). In addition, global gene expression data have shown promise in generating hypotheses about early onset “toxicity triggers” (Hamadeh et al., 2010). Topotecan is a particularly difficult drug to use in combination because of the need for dose attenuation when given in combination regimens. Having a method to identify the potential for enhanced bone marrow toxicity when topotecan is given in combination with a second agent would be particularly useful.

During the study, no drug-related adverse clinical signs were observed for any animals treated with topotecan or oxaliplatin alone or in combination. Histopathological evaluation of bone marrow established the presence of drug-related lesions in bone marrow (hypocellularity) in animals administered topotecan or oxaliplatin. Although our preclinical results highlight the need to consider the sequence of administration in a clinical protocol, our histopathological findings were not consistent with the sequence dependency of the severity of bone marrow toxicity that was reported in clinical studies of cisplatin and topotecan (de Jonge et al., 2000). In clinical trials, both neutropenia and thrombocytopenia were more severe when cisplatin was administered prior to topotecan and there were significantly lower absolute neutrophil count nadirs and percentage decrements in neutrophil and platelet counts with this sequence. Our results are consistent with the observation that oxaliplatin exhibits a favorable toxicity profile with a substantially lower incidence and severity of nephrotoxicity, ototoxicity, and myelosuppression.

Topotecan and other anticancer agents may cause DNA damage via mechanisms other than direct binding to DNA replication machinery. For example, camptothecin and analogs have been reported to induce apoptosis through a mechanism involving reactive oxygen species and oxidative stress pathways (Li et al., 2009). Similarly, pretreatment of mice with the anti-oxidant quercetin was reported to reduce topotecan-induced genotoxicity and cytotoxicity (Bakheet, 2011). Quercetin also reduced oxidative stress markers in topotecan treated bone marrow cells (Bakheet, 2011). Thus, it is feasible that the early effects of topotecan we observed in bone marrow are related to oxidative stress. Although it is clear that most of the *in vivo* biology for topotecan would be expected to be mediated by TOP1, the observed enrichment of genes related to ROS neutrophil-mediated cell damage and hypoxia-induced mitochondrial damage pathways, support additional mechanistic possibilities.

Traditional gene expression analysis has used two samples statistical tests for each comparison of interest or analysis of variance (ANOVA) model when the data are from studies with a factorial design. Upon selecting differentially expressed genes (DEGs), the next step is usually pooling the lists of DEGs to cluster analyze the data for visualization of patterns of gene expression across the samples. A limitation to this strategy is that the process of selecting the genes before detecting the patterns can omit genes that have

391 salient expression profiles correlated across the samples. This caveat is of major concern when analyzing
392 expression data comprised of genes whose expression are altered at low drug exposures or perturbed only
393 for a short duration. The EPIG approach (Chou et al., 2007) was developed specifically for toxicogenomics
394 and other series type studies where the algorithm uses an ANOVA-like statistical evaluation of the patterns
395 of gene expression but also takes into account correlation of genes within an expression pattern. In the
396 EPIG two-step approach, all significant patterns in the data are extracted first, followed by categorization of
397 gene expression profiles.

398
399 Application of the EPIG method to our microarray data and subsequent pathway and gene regulatory
400 network analyses allowed identification of genes, pathways and regulatory interactions that appear to
401 represent promising biomarker signatures for bonemarrow toxicity. Pathways related to p53 signaling,
402 DNA repair, histone biology, cell cycle regulation, hypoxia, glutathione metabolism, and respiratory and
403 oxidative phosphorylation reflect the biological effects of either treatment on the bone marrow. The
404 considerable enrichment of pathways involved with DNA repair and chromatin remodeling is remarkably
405 well-aligned with the biological mechanisms and downstream effects of topotecan. The interplay between
406 chromatin remodeling and DNA repair factors is infrequently discussed in relation to DNA damage
407 response mechanisms of the bone marrow. Our analysis highlights a meaningful relationship between
408 chromatin remodeling complexes and mechanisms of bone marrow toxicity and repair that warrants further
409 investigation.

410
411 An interesting biological response pathway of genes related to tissue injury was derived from our analysis
412 of co-expressed genes (Supplementary Table 1). Regulation of chondrogenesis, bone repair, and
413 differentiation was identified for some of the genes that were profoundly increased in response to
414 combination treatment when compared to individual treatments. These genes were matrix metalloproteinase
415 12 (MMP12); transgelin (TAGLN, SM22 α); cyclin D1 (CCND1); serpin peptidase inhibitor, clade H (heat
416 shock protein 47), member 1 (collagen binding protein1) (SERPINH1); tenascin C (TNC); ADAM
417 metalloproteinase with thrombospondin type 1 motif, 9 (ADAMTS9); and bone morphogenetic protein 2
418 (BMP2). TNC is an extracellular matrix glycoprotein that is specifically and transiently expressed upon
419 tissue injury. SERPINH1 functions as a molecular chaperone during collagen synthesis and maturation
420 (Nagata, 1998; Lamande and Bateman, 1999; Razzaque and Taguchi, 1999; Hendershot and Bulleid, 2000).
421 Upon tissue damage, TNC regulates a wide variety of pathways that mediate both inflammatory and fibrotic
422 processes, enabling effective tissue repair (Truong et al., 1996; Chiquet-Ehrismann and Chiquet,
423 2003; Midwood and Orend, 2009). TAGLN is a shape change sensitive 22 kDa actin-binding protein of the
424 calponin family that may regulate conversion of adult bone marrow-derived mesenchymal stem cells into
425 smooth muscle cells (SMCs) and is an early marker of smooth muscle differentiation (Lawson et al., 1997).
426 Expression of ADAMTS9 was shown to be up-regulated during chondrogenic differentiation of human
427 mesenchymal stem cells (Boeuf et al., 2012)

428
429 Gene profiling of bone marrow environment cells revealed distinct expression profiles for genes encoding
430 for ADAMs and their inhibitors (Bret et al., 2011). In the current study, all cells expressed ADAMTSs
431 genes at a low level, with the exception of bone marrow stromal cells. BMP2 plays an essential role in
432 chondrocyte proliferation and maturation during endochondral bone development (Shu et al., 2011).
433 Similarly, MMPs are required for both endochondral and intramembranous ossification during bone repair
434 and it is likely that this gene response is a sensitive indicator of initial degradation of extracellular matrix.
435 These gene responses are similar to microarray studies that identified gene responses during stages of bone
436 marrow-ablation-induced bone regeneration (Wise et al., 2010). Taken together, the observed gene
437 responses may represent a unique biomarker panel for bone marrow that will flag early tissue damage onset
438 followed by chondrogenesis and intramembranous regeneration processes. The 11- and 7-fold increases in
439 MMP12 and TAGLN observed 24 hours post treatment with topotecan compared with a 54- and 17-fold

440 increase when topotecan treatment is given with oxaliplatin might represent an additive response for the
441 combination. The effect of treatment combinations on these responses likely reflects a change in the extent
442 of damage and response of the bone marrow to injury.
443

444 Among the genes showing the most profound decreases in response to all treatments are several genes for
445 proteins regulating shape and hemolysis of erythrocytes. We noted a 26-fold decrease in spectrin, alpha,
446 erythrocytic 1 (elliptocytosis 2) (SPTA1). Mutations in spectrin genes that render red cells deficient in
447 spectrin are associated with abnormal cytoskeletal architecture making erythrocytes susceptible to
448 hemolysis (Kakhniashvili, 2001; Broderick and Winder, 2005). A similar contribution to actin dynamics in
449 platelets has been elucidated for pleckstrin-2 (PLEK2) (Lian et al., 2009), and we report a 14-fold decrease
450 in PLEK2 mRNA in response to topotecan alone. In addition, a 9-fold decrease was noted in Ankyrin 1
451 (ANK 1), an erythrocyte membrane protein that is defective in many patients with hereditary spherocytosis,
452 a common hemolytic anemia. Taken together our results demonstrate a clear connectivity between the most
453 profoundly affected genes and the clinical adverse effect profile for topotecan. For example, a recent
454 clinical study designed to determine the dose of weekly oral topotecan allowing safe administration in
455 patients with recurrent gynecologic malignancies, 13 (11.1%) doses of drug were held because of anemia in
456 8 patients, neutropenia in 7, or thrombocytopenia in 2 (von Gruenigen et al., 2012).
457

458 This study reports gene response data in bone marrow post treatment with topotecan or oxaliplatin alone and
459 in combination following a single administration. There are no comparable gene expression studies on the
460 effect of the combination of the two agents used here, but one study, based on 8mg/kg oxaliplatin in rat
461 bone marrow at 24-hours, was found in a public data source. That public (yet unpublished) study is
462 deposited in the Drug Matrix 8.0 database (Ganter et al., 2005) hosted by the NIEHS/NTP at
463 <https://ntp.niehs.nih.gov/drugmatrix/index.html>. One published study compares the effect of
464 oxaliplatin in ovarian cancer spheroids (L'Esperance et al., 2008). This underscores the uniqueness and
465 novel aspect of our combination study. Supplementary Figure 4 and Supplementary Figure 5 show the
466 paucity of overlap of the oxaliplatin DEGs from our current study and those from the aforementioned public
467 studies (Drug Matrix bone marrow and ovarian cancer spheroids respectively). Caution is needed in
468 interpreting these comparisons due to the differences in the doses administered, the target cell type/tissue,
469 the array platforms, significance test and the annotations based on gene symbol to compare results. We
470 provide a comprehensive list of genes from our microarray analysis of bone marrow taken at various time
471 points after treatment of rats to enable additional analysis and hypothesis generation
472 (<http://tools.niehs.nih.gov/cebs3/ui/>). Although we will continue to analyze these data for biological
473 response pathways and mechanistic pathways for toxicity, we publish these data to encourage other
474 investigators to employ alternative analysis methods and propose additional relationships relevant to the
475 observed bone marrow responses and treatments.
476

477 The use of a single dose study using genomic endpoints as a measure of enhanced bone marrow toxicity is
478 exciting for several reasons. This approach could be incorporated into a mechanism-based risk evaluation
479 and a single dose administration can be readily incorporated as an *in vivo* or *in vitro* screening paradigm.
480 For example, attempts to validate *in vitro* bone marrow systems could use these data to explore and identify
481 molecular anchors that translate from *in vitro* to *in vivo*. Second, this proof of concept revealed that the
482 molecular responses in bone marrow toxicity is much earlier than previously documented preclinical
483 histopathological observations of topotecan toxicity. Examining the acute response of a target organ to
484 chemotherapy and obtaining a molecular footprint associated with this response in combination with a
485 targeted agent can guide us along new avenues of investigation about mechanisms of target-mediated
486 toxicity. At this point, these data represent qualitative information that is relevant to understanding
487 mechanisms of toxicity. The initial phenotypic anchoring of these data with additional endpoints may
488 ultimately provide a more comprehensive understanding of pathways underlying bone marrow toxicities.

489 Indeed, other reports have highlighted the potential use of toxicogenomics data to enable integrative risk
490 assessment and biomarker identification (Ellinger-Ziegelbauer et al., 2011;Matheis et al., 2011). We plan to
491 apply this approach to other target organs and additional anticancer drug combinations to examine the
492 broader implications of this strategy.

493
494
495 **Conflict of Interest Statement**

496
497 The authors disclose no potential conflicts of interest.
498

Acknowledgement

The Authors would like to acknowledge the editorial assistance of Melinie Simpson.

The content of this publication does not necessarily reflect the views or policies of the Department of Health and Human Services, nor does mention of trade names, commercial products, or organizations imply endorsement by the U.S. Government. This research was supported in part by the Developmental Therapeutics Program in the Division of Cancer Treatment and Diagnosis of the National Cancer Institute and the National Institute of Environmental Health Sciences.

References

- Alexandre, J., Tigaud, J.M., Gross-Goupil, M., Gornet, J.M., Romain, D., Azoulay, D., Misset, J.L., and Goldwasser, F. (2002). Combination of topotecan and oxaliplatin in inoperable hepatocellular cancer patients. *Am J Clin Oncol* 25, 198-203.
- Bakheet, S.A. (2011). Assessment of anti-cytogenotoxic effects of quercetin in animals treated with topotecan. *Oxid Med Cell Longev* 2011, 824597.
- Barrett, T., Wilhite, S.E., Ledoux, P., Evangelista, C., Kim, I.F., Tomashevsky, M., Marshall, K.A., Phillippy, K.H., Sherman, P.M., Holko, M., Yefanov, A., Lee, H., Zhang, N., Robertson, C.L., Serova, N., Davis, S., and Soboleva, A. (2013). NCBI GEO: archive for functional genomics data sets--update. *Nucleic Acids Res* 41, D991-995.
- Boeuf, S., Graf, F., Fischer, J., Moradi, B., Little, C.B., and Richter, W. (2012). Regulation of aggrecanases from the ADAMTS family and aggrecan neoepitope formation during in vitro chondrogenesis of human mesenchymal stem cells. *Eur Cell Mater* 23, 320-332.
- Bret, C., Hose, D., Reme, T., Kassambara, A., Seckinger, A., Meissner, T., Schved, J.F., Kanouni, T., Goldschmidt, H., and Klein, B. (2011). Gene expression profile of ADAMs and ADAMTS metalloproteinases in normal and malignant plasma cells and in the bone marrow environment. *Exp Hematol* 39, 546-557 e548.
- Broderick, M.J.F., and Winder, S.J. (2005). "Spectrin, α -Actinin, and Dystrophin," in *Advances in Protein Chemistry*, eds. A.D.P. David & M.S. John. Academic Press), 203-246.
- Bushel, P.R., Heinloth, A.N., Li, J., Huang, L., Chou, J.W., Boorman, G.A., Malarkey, D.E., Houle, C.D., Ward, S.M., Wilson, R.E., Fannin, R.D., Russo, M.W., Watkins, P.B., Tennant, R.W., and Paules, R.S. (2007). Blood gene expression signatures predict exposure levels. *Proc Natl Acad Sci U S A* 104, 18211-18216.
- Chengalvala, M.V., Chennathukuzhi, V.M., Johnston, D.S., Stevis, P.E., and Kopf, G.S. (2007). Gene expression profiling and its practice in drug development. *Curr Genomics* 8, 262-270.
- Chiquet-Ehrismann, R., and Chiquet, M. (2003). Tenascins: regulation and putative functions during pathological stress. *J Pathol* 200, 488-499.
- Chou, J.W., Zhou, T., Kaufmann, W.K., Paules, R.S., and Bushel, P.R. (2007). Extracting gene expression patterns and identifying co-expressed genes from microarray data reveals biologically responsive processes. *BMC Bioinformatics* 8, 427.
- De Jonge, M.J., Loos, W.J., Gelderblom, H., Planting, A.S., Van Der Burg, M.E., Sparreboom, A., Brouwer, E., Van Beurden, V., Mantel, M.A., Doyle, E., Hearn, S., Ross, G., and Verweij, J. (2000). Phase I pharmacologic study of oral topotecan and intravenous cisplatin: sequence-dependent hematologic side effects. *J Clin Oncol* 18, 2104-2115.
- Edgar, R., Domrachev, M., and Lash, A.E. (2002). Gene Expression Omnibus: NCBI gene expression and hybridization array data repository. *Nucleic Acids Res* 30, 207-210.

- Elkas, J.C., Winter, W.E., 3rd, Chernofsky, M.R., Sunde, J., Bidus, M.A., Bernstein, S., and Rose, G.S. (2007). A phase I trial of oxaliplatin and topotecan in recurrent ovarian carcinoma. *Gynecol Oncol* 104, 422-427.
- Ellinger-Ziegelbauer, H., Adler, M., Amberg, A., Brandenburg, A., Callanan, J.J., Connor, S., Fountoulakis, M., Gmuender, H., Gruhler, A., Hewitt, P., Hodson, M., Matheis, K.A., McCarthy, D., Raschke, M., Riefke, B., Schmitt, C.S., Sieber, M., Sposny, A., Suter, L., Sweatman, B., and Mally, A. (2011). The enhanced value of combining conventional and "omics" analyses in early assessment of drug-induced hepatobiliary injury. *Toxicol Appl Pharmacol* 252, 97-111.
- Fda, C.F.D.E.a.R. (2002). "Pharmacology Review".).
- Friberg, L.E., Henningsson, A., Maas, H., Nguyen, L., and Karlsson, M.O. (2002). Model of chemotherapy-induced myelosuppression with parameter consistency across drugs. *J Clin Oncol* 20, 4713-4721.
- Ganter, B., Tugendreich, S., Pearson, C.I., Ayanoglu, E., Baumhueter, S., Bostian, K.A., Brady, L., Browne, L.J., Calvin, J.T., Day, G.J., Breckenridge, N., Dunlea, S., Eynon, B.P., Furness, L.M., Ferng, J., Fielden, M.R., Fujimoto, S.Y., Gong, L., Hu, C., Idury, R., Judo, M.S., Kolaja, K.L., Lee, M.D., Mcsorley, C., Minor, J.M., Nair, R.V., Natsoulis, G., Nguyen, P., Nicholson, S.M., Pham, H., Roter, A.H., Sun, D., Tan, S., Thode, S., Tolley, A.M., Vladimirova, A., Yang, J., Zhou, Z., and Jarnagin, K. (2005). Development of a large-scale chemogenomics database to improve drug candidate selection and to understand mechanisms of chemical toxicity and action. *J Biotechnol* 119, 219-244.
- Ganter, B., Zidek, N., Hewitt, P.R., Muller, D., and Vladimirova, A. (2008). Pathway analysis tools and toxicogenomics reference databases for risk assessment. *Pharmacogenomics* 9, 35-54.
- Gentleman, R. (2005). *Bioinformatics and computational biology solutions using R and Bioconductor*. New York ; Cambridge: Springer.
- Goldwasser, F., Bozec, L., Zeghari-Squalli, N., and Misset, J.L. (1999). Cellular pharmacology of the combination of oxaliplatin with topotecan in the IGROV-1 human ovarian cancer cell line. *Anticancer Drugs* 10, 195-201.
- Guerreiro, N., Staedtler, F., Grenet, O., Kehren, J., and Chibout, S.D. (2003). Toxicogenomics in drug development. *Toxicol Pathol* 31, 471-479.
- Hamadeh, H.K., Todd, M., Healy, L., Meyer, J.T., Kwok, A.M., Higgins, M., and Afshari, C.A. (2010). Application of genomics for identification of systemic toxicity triggers associated with VEGF-R inhibitors. *Chem Res Toxicol* 23, 1025-1033.
- Hendershot, L.M., and Bulleid, N.J. (2000). Protein-specific chaperones: the role of hsp47 begins to gel. *Curr Biol* 10, R912-915.
- Huang, J., Shi, W., Zhang, J., Chou, J.W., Paules, R.S., Gerrish, K., Li, J., Luo, J., Wolfinger, R.D., Bao, W., Chu, T.M., Nikolsky, Y., Nikolskaya, T., Dosymbekov, D., Tsyganova, M.O., Shi, L., Fan, X., Corton, J.C., Chen, M., Cheng, Y., Tong, W., Fang, H., and Bushel, P.R. (2010). Genomic indicators in the blood predict drug-induced liver injury. *Pharmacogenomics J* 10, 267-277.
- Irizarry, R.A., Bolstad, B.M., Collin, F., Cope, L.M., Hobbs, B., and Speed, T.P. (2003a). Summaries of Affymetrix GeneChip probe level data. *Nucleic Acids Res* 31, e15.

- Irizarry, R.A., Hobbs, B., Collin, F., Beazer-Barclay, Y.D., Antonellis, K.J., Scherf, U., and Speed, T.P. (2003b). Exploration, normalization, and summaries of high density oligonucleotide array probe level data. *Biostatistics* 4, 249-264.
- Kakhniashvili (2001). Erythrocyte Spectrin Is an E2 Ubiquitin Conjugating Enzyme†. *Biochemistry* 40, 11630-11642.
- Kelder, T., Van Iersel, M.P., Hanspers, K., Kutmon, M., Conklin, B.R., Evelo, C.T., and Pico, A.R. (2012). WikiPathways: building research communities on biological pathways. *Nucleic Acids Res* 40, D1301-1307.
- Kummar, S., Chen, H.X., Wright, J., Holbeck, S., Millin, M.D., Tomaszewski, J., Zweibel, J., Collins, J., and Doroshow, J.H. (2010). Utilizing targeted cancer therapeutic agents in combination: novel approaches and urgent requirements. *Nat Rev Drug Discov* 9, 843-856.
- L'esperance, S., Bachvarova, M., Tetu, B., Mes-Masson, A.M., and Bachvarov, D. (2008). Global gene expression analysis of early response to chemotherapy treatment in ovarian cancer spheroids. *BMC Genomics* 9, 99.
- Lamande, S.R., and Bateman, J.F. (1999). Procollagen folding and assembly: the role of endoplasmic reticulum enzymes and molecular chaperones. *Semin Cell Dev Biol* 10, 455-464.
- Lawson, D., Harrison, M., and Shapland, C. (1997). Fibroblast transgelin and smooth muscle SM22alpha are the same protein, the expression of which is down-regulated in many cell lines. *Cell Motil Cytoskeleton* 38, 250-257.
- Li, Y., Rory Goodwin, C., Sang, Y., Rosen, E.M., Laterra, J., and Xia, S. (2009). Camptothecin and Fas receptor agonists synergistically induce medulloblastoma cell death: ROS-dependent mechanisms. *Anticancer Drugs* 20, 770-778.
- Lian, L., Wang, Y., Flick, M., Choi, J., Scott, E.W., Degen, J., Lemmon, M.A., and Abrams, C.S. (2009). Loss of pleckstrin defines a novel pathway for PKC-mediated exocytosis. *Blood* 113, 3577-3584.
- Matheis, K.A., Com, E., Gautier, J.C., Guerreiro, N., Brandenburg, A., Gmuender, H., Sposny, A., Hewitt, P., Amberg, A., Boernsen, O., Riefke, B., Hoffmann, D., Mally, A., Kalkuhl, A., Suter, L., Dieterle, F., and Staedtler, F. (2011). Cross-study and cross-omics comparisons of three nephrotoxic compounds reveal mechanistic insights and new candidate biomarkers. *Toxicol Appl Pharmacol* 252, 112-122.
- Midwood, K.S., and Orend, G. (2009). The role of tenascin-C in tissue injury and tumorigenesis. *J Cell Commun Signal* 3, 287-310.
- Nagata, K. (1998). Expression and function of heat shock protein 47: a collagen-specific molecular chaperone in the endoplasmic reticulum. *Matrix Biol* 16, 379-386.
- Nuwaysir, E.F., Bittner, M., Trent, J., Barrett, J.C., and Afshari, C.A. (1999). Microarrays and toxicology: the advent of toxicogenomics. *Mol Carcinog* 24, 153-159.
- Razzaque, M.S., and Taguchi, T. (1999). The possible role of colligin/HSP47, a collagen-binding protein, in the pathogenesis of human and experimental fibrotic diseases. *Histol Histopathol* 14, 1199-1212.

- Ruepp, S., Boess, F., Suter, L., De Vera, M.C., Steiner, G., Steele, T., Weiser, T., and Albertini, S. (2005). Assessment of hepatotoxic liabilities by transcript profiling. *Toxicol Appl Pharmacol* 207, 161-170.
- Ryan, T.P., Stevens, J.L., and Thomas, C.E. (2008). Strategic applications of toxicogenomics in early drug discovery. *Curr Opin Pharmacol* 8, 654-660.
- Segura, C., Bandres, E., Troconiz, I.F., Garcia-Foncillas, J., Sayar, O., Dios-Vieitez, C., Renedo, M.J., and Garrido, M.J. (2004). Hematological response of topotecan in tumor-bearing rats: modeling of the time course of different cellular populations. *Pharm Res* 21, 567-573.
- Shu, B., Zhang, M., Xie, R., Wang, M., Jin, H., Hou, W., Tang, D., Harris, S.E., Mishina, Y., O'keefe, R.J., Hilton, M.J., Wang, Y., and Chen, D. (2011). BMP2, but not BMP4, is crucial for chondrocyte proliferation and maturation during endochondral bone development. *J Cell Sci* 124, 3428-3440.
- Smyth, G. (2005). Limma: linear models for microarray data. *Bioinformatics and Computational Biology Solutions using R and Bioconductor*, 397-420.
- Subramanian, A., Tamayo, P., Mootha, V.K., Mukherjee, S., Ebert, B.L., Gillette, M.A., Paulovich, A., Pomeroy, S.L., Golub, T.R., Lander, E.S., and Mesirov, J.P. (2005). Gene set enrichment analysis: a knowledge-based approach for interpreting genome-wide expression profiles. *Proc Natl Acad Sci U S A* 102, 15545-15550.
- Tortora, G., Ciardiello, F., Damiano, V., De Laurentiis, M., Matano, E., Pepe, S., Pensabene, M., Catalano, G., De Placido, S., and Bianco, A.R. (2002). Preclinical and phase I study of oxaliplatin and topotecan in combination in human cancer. *Ann Oncol* 13, 392-398.
- Truong, L.D., Foster, S.V., Barrios, R., D'agati, V., Verani, R.R., Gonzalez, J.M., and Suki, W.N. (1996). Tenascin is an ubiquitous extracellular matrix protein of human renal interstitium in normal and pathologic conditions. *Nephron* 72, 579-586.
- Van Iersel, M.P., Kelder, T., Pico, A.R., Hanspers, K., Coort, S., Conklin, B.R., and Evelo, C. (2008). Presenting and exploring biological pathways with PathVisio. *BMC Bioinformatics* 9, 399.
- Von Gruenigen, V.E., Frasure, H.E., Smith, D.A., Fusco, N.L., Eaton, S.M., Debernardo, R.L., Heugel, A.M., and Waggoner, S.E. (2012). Toxicity of weekly oral topotecan in relation to dosage for gynecologic malignancies: a phase I study. *Anticancer Drugs* 23, 724-730.
- Wang, Y., Joshi, T., Zhang, X.S., Xu, D., and Chen, L. (2006). Inferring gene regulatory networks from multiple microarray datasets. *Bioinformatics* 22, 2413-2420.
- Waters, M., Stasiewicz, S., Merrick, B.A., Tomer, K., Bushel, P., Paules, R., Stegman, N., Nehls, G., Yost, K.J., Johnson, C.H., Gustafson, S.F., Xirasagar, S., Xiao, N., Huang, C.C., Boyer, P., Chan, D.D., Pan, Q., Gong, H., Taylor, J., Choi, D., Rashid, A., Ahmed, A., Howle, R., Selkirk, J., Tennant, R., and Fostel, J. (2008). CEBS--Chemical Effects in Biological Systems: a public data repository integrating study design and toxicity data with microarray and proteomics data. *Nucleic Acids Res* 36, D892-900.
- Wise, J.K., Sena, K., Vranizan, K., Pollock, J.F., Healy, K.E., Hughes, W.F., Sumner, D.R., and Viridi, A.S. (2010). Temporal gene expression profiling during rat femoral marrow ablation-induced intramembranous bone regeneration. *PLoS One* 5.

Table 1. Study Design

Group	Treatment	Dose of Topotecan (mg/kg)	Dose of Oxaliplatin (mg/kg)	No. Animals per Group	No. Animals per Necropsy Time point (Hours)		
					1	6	24
1	0.9% NaCl (30 min infusion) followed by D5W (30 min infusion)	0	0	12	4	4	4
2	D5W (30 min infusion) followed by 0.9% NaCl (30 min infusion)	0	0	12	4	4	4
3	Topotecan (30 min infusion) followed by D5W (30 min infusion)	4.7 (<i>first infusion</i>)	0	12	4	4	4
4	Oxaliplatin (30 min infusion) followed by 0.9% NaCl (30 min infusion)	0	15 (<i>first infusion</i>)	12	4	4	4
5	Topotecan (30 min infusion) followed by Oxaliplatin (30 min infusion)	4.7 (<i>first infusion</i>)	15 (<i>second infusion</i>)	12	4	4	4
6	Oxaliplatin (30 min infusion) followed by Topotecan (30 min infusion)	4.7 (<i>second infusion</i>)	15 (<i>first infusion</i>)	12	4	4	4
7	0.9% NaCl (30 min infusion) followed by Oxaliplatin (30 min infusion)	0	15 (<i>second infusion</i>)	12	4	4	4
8	D5W (30 min infusion) followed by Topotecan (30 min infusion)	4.7 (<i>second infusion</i>)	0	12	4	4	4

Table 2. Histopathology of the Bone Marrow

1 Hour Post-Dose: Severity of Test Article-Related Microscopic Lesions								
Tissue, Microscopic Lesion	0.9% saline D5W	D5W 0.9% saline	Topotecan/ D5W	Oxaliplatin 0.9% saline	Topotecan Oxaliplatin	Oxaliplatin Topotecan	0.9% saline oxaliplatin	D5W/ Topotecan
Bone marrow, hypocellularity	NA	NA	Minimal to mild	NA	Minimal	Minimal to mild	NA	Minimal
6 Hour Post-Dose: Severity of Test Article-Related Microscopic Lesions								
Tissue, Microscopic Lesion	0.9% saline D5W	D5W 0.9% saline	Topotecan D5W	Oxaliplatin 0.9% saline	Topotecan Oxaliplatin	Oxaliplatin Topotecan	0.9% saline oxaliplatin	D5W Topotecan
Bone marrow, hypocellularity	NA	NA	Minimal to mild	Minimal to mild	Minimal to mild	Mild	Minimal to mild	Minimal to mild
24 Hour Post-Dose: Severity of Test Article-Related Microscopic Lesions								
Tissue, Microscopic Lesion	0.9% saline D5W	D5W 0.9% saline	Topotecan D5W	Oxaliplatin 0.9% saline	Topotecan Oxaliplatin	Oxaliplatin Topotecan	0.9% saline oxaliplatin	D5W Topotecan
Bone marrow, hypocellularity	NA	NA	Mild	Minimal to mild	Mild to moderate	Mild to moderate	Minimal to mild	Mild to moderate

Table 3. List of Representative Pattern-Specific Genes Showing at Least Four-fold Increase from Their Respective Controls 24 hours after treatment.

group	Symbol	Entrez Gene Name	Pattern Number	Control DSW	Control NaCl	Topotecan followed by DSW	Oxaliplatin followed by NaCl	Topotecan followed by Oxaliplatin	Oxaliplatin followed by Topotecan	NaCl followed by Oxaliplatin	DSW followed by Topotecan
1368530_at	MMP12	matrix metalloproteinase 12 (macrophage elastase)	1	0.49	-0.33	11.57	15.11	54.72	31.26	12.98	22.82
1376908_at	IFIT3	interferon-induced protein with tetratricopeptide repeats 3	1	0.00	-0.33	10.34	10.21	30.05	16.47	5.87	7.95
1367570_at	TAGLN	transgelin	1	0.00	-0.33	6.92	5.81	17.71	12.09	8.80	9.15
1373401_at	TNC	tenascin C	1	0.49	0.32	6.80	6.61	8.27	5.43	7.75	5.86
1367712_at	TIMP1	TIMP metalloproteinase inhibitor 1	3	-0.49	0.33	6.51	3.30	14.33	9.40	4.19	8.14
1371310_s_at	SERPINH1	serpin peptidase inhibitor, clade H (heat shock protein 47)	1	0.50	0.33	5.54	5.21	9.29	7.71	5.97	6.57
1383075_at	CEND1	cyclin D1	1	0.00	0.33	5.44	5.58	8.49	5.51	3.75	5.80
1376481_at	ADAMTS9	ADAM metalloproteinase with thrombospondin type 1 motif, 9	1	0.49	0.33	5.16	5.92	8.68	8.22	5.02	7.36
1373463_at	COL5A2	collagen, type V, alpha 2	1	0.49	-0.33	5.14	3.86	6.21	6.08	4.07	4.21
1367973_at	CCl13	chemokine (C-C motif) ligand 13	3	0.00	0.29	4.74	4.85	17.18	11.17	5.79	6.04
1379285_at	RTP4	receptor (chemosensory) transporter protein 4	2	0.00	-0.33	4.69	4.38	11.12	6.45	2.87	4.48
1387232_at	BMP4	bone morphogenetic protein 4	1	-0.50	0.33	4.55	5.68	9.16	9.33	5.62	7.72
1383564_at	IRF7	interferon regulatory factor 7	2	0.00	0.33	4.53	3.68	9.57	5.05	3.07	3.42
1387197_at	OMD	osteoinductin	1	0.00	-0.33	4.47	3.53	7.12	4.44	4.24	3.91
1370895_at	COL5A2	collagen, type V, alpha 2	1	0.49	-0.33	4.43	3.56	5.52	5.28	3.97	3.66
1376845_at	IFI27L2	interferon, alpha-inducible protein 27-like 2	2	-0.42	-0.33	4.42	7.44	15.15	9.46	4.73	7.69
1367691_at	PRKCDBP	protein kinase C, delta binding protein	1	0.50	0.33	4.42	5.43	9.95	8.03	5.36	7.07
1367896_at	CA3	carbonic anhydrase III, muscle specific	1	-0.10	-0.33	4.42	7.77	6.69	8.67	5.15	9.88
1368059_at	CRYM	crystallin, mu	1	0.50	-0.33	4.32	5.72	8.54	7.70	5.05	7.17
1371643_at	CEND1	cyclin D1	1	0.00	-0.33	4.26	4.95	7.26	5.49	3.94	5.16
1367562_at	SPARC	secreted protein, acidic, cysteine-rich (osteonectin)	1	-0.01	0.33	4.26	3.19	5.15	3.47	3.97	2.96
1398270_at	BMP2	bone morphogenetic protein 2	1	0.00	-0.33	4.18	5.49	9.56	8.44	5.10	5.35
1388569_at	SERPINF1	serpin peptidase inhibitor, clade F, member 1	1	0.00	0.33	3.85	3.30	5.44	4.30	3.92	3.36
1380912_at	PCOLCE	procollagen C-endopeptidase enhancer	1	0.00	0.33	3.85	4.21	7.72	6.44	4.35	5.15
1386884_at	HTRA1	HTRA serine peptidase 1	1	0.00	0.33	3.71	3.50	6.86	4.71	3.74	4.66
1388439_at	FKBP10	FK506 binding protein 10, 65 kDa	1	0.00	0.33	3.31	2.87	4.27	3.71	3.22	3.32
1377367_at	KAZALD1	Kazal-type serine peptidase inhibitor domain 1	1	0.00	-0.33	3.30	3.40	5.51	4.99	2.99	4.64
1389918_at	PALLD	palladin, cytoskeletal associated protein	1	0.01	-0.33	3.28	3.53	5.88	5.98	2.97	3.78
1373674_at	MFAP5	microfibrillar associated protein 5	1	0.01	0.33	3.27	4.42	4.65	4.51	4.51	5.44
1384180_at	IFIT2	interferon-induced protein with tetratricopeptide repeats 2	2	0.00	0.33	3.22	4.21	7.22	4.67	2.60	2.59
1386977_at	CA3	carbonic anhydrase III, muscle specific	1	-0.01	-0.33	3.20	6.20	5.83	7.29	4.91	8.97
1386953_at	HSD11B1	hydroxysteroid (11-beta) dehydrogenase 1	1	0.00	-0.32	3.19	3.10	4.09	3.23	3.38	4.14
1372219_at	TPM2	tropomyosin 2 (beta)	1	0.00	-0.32	3.18	3.59	7.20	5.12	4.12	4.06
1387770_at	IFI27L1	interferon, alpha-inducible protein 27 like 1	5	-0.50	0.31	3.16	3.91	6.03	4.74	2.67	4.12
1370301_at	MMP2	matrix metalloproteinase 2 (gelatinase A)	1	0.00	-0.33	3.01	6.32	9.88	10.38	5.08	3.96
1393240_at	EFEMP2	EGF containing fibulin-like extracellular matrix protein 2	1	0.50	0.33	3.00	3.60	5.17	4.64	3.13	4.03
1373210_at	LAMB1	laminin, beta 1	1	0.00	-0.33	3.00	3.65	6.70	4.69	3.54	3.44
1378443_at	SLAMF9	SLAM family member 9	2	0.00	0.33	2.99	2.63	5.97	3.15	2.17	3.23
1371150_at	CEND1	cyclin D1	1	-0.50	-0.33	2.53	2.88	4.21	3.45	2.44	3.48
1390192_at	SLC27A3	solute carrier family 27 (fatty acid transporter), member 3	1	0.00	0.33	2.51	4.51	6.68	6.17	4.42	4.04
1376151_a_at	LOC100365106	CCG32755-like	5	0.00	0.33	2.50	3.22	5.37	4.85	2.01	2.73
1370927_at	COL12A1	collagen, type XII, alpha 1	1	0.00	0.33	2.49	2.88	4.25	3.39	2.63	2.69
1369665_a_at	IL18	interleukin 18 (interferon-gamma-inducing factor)	3	0.00	-0.33	2.49	2.05	4.05	2.57	2.13	2.60
1387259_at	CDH2	cadherin 2, type 1, N-cadherin (neuronal)	1	0.00	-0.33	2.47	2.95	4.16	4.45	2.61	3.49
1383266_at	SFRP1	secreted frizzled-related protein 1	1	-0.50	-0.33	2.46	2.66	4.50	2.99	2.68	2.95
1369720_at	MYO18	myosin 18	1	0.00	-0.33	2.46	2.79	4.98	4.42	3.66	2.74
1387394_at	IL2RB	interleukin 2 receptor, beta	5	-0.50	0.33	2.42	2.85	4.26	5.07	2.57	2.99
1397304_at	Igtp	interferon gamma induced GTPase	5	0.00	0.33	2.40	3.15	5.91	4.46	2.26	2.80
1384182_at	FERMT2	fermitin family member 2	1	0.00	0.33	2.40	2.92	4.27	4.10	2.91	3.26
1372439_at	COL4A1	collagen, type IV, alpha 1	1	0.00	0.33	2.40	3.21	5.98	4.10	3.39	3.26
1375377_at	IGSF3	immunoglobulin superfamily, member 3	1	0.00	0.33	2.39	2.91	4.50	4.43	3.20	3.33
1376706_at	TMEM47	transmembrane protein 47	1	0.50	-0.33	2.38	3.00	4.58	4.23	2.85	3.15
1380965_at	LPL	lipoprotein lipase	1	0.00	0.33	2.38	6.33	6.04	6.35	3.96	5.18
1369640_at	GJA1	gap junction protein, alpha 1, 43kDa	1	0.00	0.33	2.37	2.87	4.74	4.37	3.94	3.43
1387122_at	PLAGL1	pleiomorphic adenoma gene-like 1	1	0.00	0.33	2.36	2.79	4.26	3.79	2.04	3.04
1387015_at	Pfn2	profilin 2	1	0.00	0.33	2.36	2.62	5.68	4.42	3.01	3.69
1372064_at	CXCL16	chemokine (C-X-C motif) ligand 16	3	0.00	-0.33	2.35	2.30	5.27	3.64	2.05	2.52
1368961_at	MMP23B	matrix metalloproteinase 23B	1	0.50	-0.33	2.35	3.09	5.94	5.17	3.36	3.90
1382192_at	LVE1	lymphatic vessel endothelial hyaluronan receptor 1	3	0.00	0.32	2.35	2.60	5.04	4.09	2.23	3.53
1370167_at	SDC2	syndecan 2	1	0.00	-0.33	2.35	2.69	4.25	3.66	3.11	3.12
1370244_at	CTS1	cathepsin L2	1	-0.50	-0.33	2.33	2.45	4.55	3.07	3.22	2.84
1370333_a_at	IGF1	insulin-like growth factor 1 (somatomedin C)	3	-0.50	-0.33	2.32	1.82	4.08	2.97	2.80	3.18
1376198_at	CLMP	CXADR-like membrane protein	1	0.00	0.33	2.32	2.84	4.28	4.22	2.71	3.36
1368945_at	BMP2	bone morphogenetic protein 2	1	0.00	0.33	2.32	2.34	4.12	3.09	2.96	2.18
1388856_at	KITLG	KIT ligand	1	0.00	0.32	2.32	2.98	4.35	4.03	3.46	3.46
1391489_at	IRGM	immunity-related GTPase family, M	2	0.00	0.33	2.31	2.23	5.14	3.41	1.88	2.23
1370959_at	COL3A1	collagen, type III, alpha 1	1	0.00	0.32	2.31	3.36	5.34	4.36	2.85	3.42
1384392_at	CYP26B1	cytochrome P450, family 26, subfamily B, polypeptide 1	1	0.00	0.33	2.31	3.28	6.54	5.60	3.08	2.17
1392265_s_at	MMP23B	matrix metalloproteinase 23B	1	0.00	0.33	2.29	2.49	6.16	4.13	2.81	3.65
1376920_at	LOC500013	similar to sterile alpha motif domain containing 9-like	5	0.00	0.33	2.27	3.04	4.17	3.63	2.06	2.30
1387455_a_at	VLDLR	very low density lipoprotein receptor	3	0.00	0.33	2.26	2.04	5.29	3.14	2.69	3.11
1394022_at	ID4	inhibitor of DNA binding 4, dominant negative helix-loop-helix protein	1	-0.50	-0.33	2.25	2.38	4.11	3.18	2.70	2.12
1387995_a_at	Ifitm3	interferon induced transmembrane protein 3	2	0.00	-0.33	2.24	2.48	5.15	3.34	2.59	2.32
1385248_a_at	OGN	osteoglycin	1	0.48	0.33	2.24	3.20	8.01	3.97	4.86	3.37
1387472_at	CD3D	CD3d molecule, delta (CD3-TCR complex)	5	-0.50	-0.33	2.24	2.76	4.40	4.32	2.86	2.95
1377340_at	TFPI2	tissue factor pathway inhibitor 2	3	0.00	-0.33	2.24	2.54	4.71	2.97	2.73	2.96
1368821_at	FSTL1	folliculin-like 1	1	-0.50	0.33	2.23	2.61	5.00	4.11	3.62	3.47
1370950_at	PPAP2B	phosphatidic acid phosphatase type 2B	1	0.00	0.33	2.22	2.99	4.24	3.99	2.88	2.97
1371369_at	COL6A2	collagen, type VI, alpha 2	1	0.50	0.33	2.20	2.59	4.19	3.50	2.73	2.55
1374496_at	TRIL	TLR4 interactor with leucine-rich repeats	1	0.50	0.33	2.17	2.31	4.83	3.45	2.67	2.49
1389546_at	AMOTL2	angiostatin-like 2	1	0.50	-0.33	2.17	4.01	5.02	5.11	3.38	3.23
1372101_at	PPAP2B	phosphatidic acid phosphatase type 2B	1	0.00	-0.33	2.17	3.14	4.13	3.85	2.99	2.95
1389651_at	APLN	apelin	1	-0.50	-0.33	2.16	4.39	8.56	7.82	5.02	2.93
1369207_at	IL7	interleukin 7	1	-0.50	-0.33	2.00	2.30	4.07	2.88	2.63	2.86
1390075_at	OLFML2B	olfactomedin-like 2B	1	0.00	-0.33	2.00	3.19	5.15	3.83	3.06	3.20
1372587_at	EMCN	endomucin	1	0.00	-0.33	1.98	2.43	4.16	2.74	2.99	2.33
1370202_at	PLA2G16	phospholipase A2, group XVI	3	0.00	-0.32	1.97	2.03	4.05	2.80	2.12	2.31
1368702_at	PAWR	PRKC, apoptosis, WT1, regulator	3	0.50	-0.33	1.96	1.97	4.35	3.14	2.01	2.48
1371349_at	COL6A1	collagen, type VI, alpha 1	1	0.00	-0.33	1.96	2.33	4.00	3.48	2.58	2.42
1376106_at	TMEM178	transmembrane protein 178	1	0.00	0.33	1.96	2.84	5.12	4.75	2.60	3.70
1384558_at	Plac9	placenta-specific 9	1	0.50	0.33	1.93	2.55	4.07	2.73	2.33	3.40
1390776_at	IRX3	iroquois homeobox 3	1	0.00	-0.33	1.93	2.18	4.03	3.30	2.17	2.34
1390156_a_at	PRICKLE2	prickle homolog 2 (Drosophila)	1	0.00	-0.33	1.89	2.78	4.27	4.35	2.42	2.99
1373245_at	COL4A1	collagen, type IV, alpha 1	1	0.00	-0.33	1.88	2.63	5.20	3.83	2.87	2.55
1385173_at	EBF3	early B-cell factor 3	1	0.00	0.33	1.82	3.27	4.81	5.02	3.12	3.58
1368271_a_at	FABP4	fatty acid binding protein 4, adipocyte	1	0.00	-0.32	1.81	3.13	4.89	3.66	3.99	2.95
1367774_at	Gsta3	glutathione S-transferase A3	1	0.50	-0.31	1.81	2.58	4.11	2.53	2.49	2.31
1384150_at	MID1	midline 1 (Opitz/BBB syndrome)	3	0.50	0.33	1.79	2.10	4.37	3.53	2.07	2.57
1368725_at	JAG1	jagged 1	1	-0.50	0.33	1.78	2.47	4.34	3.52	2.72	2.37
1371691_at	RARBES2	retinoic acid receptor responder (tazarotene induced) 2	1	0.00	-0.33	1.77	2.22	4.44	2.83	2.37	2.79
1375224_at	PHLDA3	pleckstrin homology-like domain, family A, member 3	1	0.00	-0.33	1.76	4.61	6.21	5.57	4.22	3.29
1378220_at	Rpl39l	ribosomal protein L39-like	3	0.50	-0.33	1.76	1.57	4.03	2.51	1.83	2.50
1369313_at	FHL2	four and a half LIM domains 2	1	0.00	-0.33						

Table 4. List of Representative Pattern-Specific Genes Showing at Least Four-fold Decrease from Their Respective Controls 24 hours after treatment.

group	Symbol	Entrez Gene Name	Pattern Number	Control D5W	Control NaCl	Topotecan followed by D5W	Oxaliplatin followed by NaCl	Topotecan followed by Oxaliplatin	Oxaliplatin followed by Topotecan	NaCl followed by Oxaliplatin	D5W followed by Topotecan
1397312_at	XPO7	exportin 7	17	0.00	-0.33	-4.00	-1.98	-4.48	-4.63	-1.84	-4.07
1377079_a_at	PPOX	protoporphyrinogen oxidase	16	0.00	-0.33	-4.02	-3.42	-4.03	-3.70	-4.17	-3.69
1376118_at	OTUB2	OTU domain, ubiquitin aldehyde binding 2	16	0.00	-0.33	-4.05	-2.76	-4.04	-3.34	-3.29	-3.24
1392512_at	Hist3h2ba	histone cluster 3, H2ba	17	0.00	-0.33	-4.05	-3.01	-3.41	-3.37	-3.00	-4.93
1389160_at	AHSP	alpha hemoglobin stabilizing protein	17	0.50	0.33	-4.05	-2.20	-4.79	-4.41	-2.48	-4.98
1383593_at	TMEM56	transmembrane protein 56	16	0.00	-0.33	-4.07	-4.83	-6.91	-4.69	-6.22	-4.36
1394361_a_at	WNT2	wingless-type MMTV integration site family member 2	17	0.48	-0.33	-4.08	-2.46	-3.98	-2.70	-3.82	-2.86
1390465_at	RNF123	ring finger protein 123	17	0.00	-0.33	-4.10	-2.58	-3.55	-2.49	-2.49	-4.20
1370878_at	UROD	uroporphyrinogen decarboxylase	16	0.00	0.33	-4.13	-3.37	-4.51	-4.31	-3.69	-4.05
1382963_at	ABCB10	ATP-binding cassette, sub-family B (MDR/TAP), member 10	16	0.00	-0.33	-4.13	-3.47	-5.65	-4.44	-3.78	-4.52
1387970_at	SLC38A5	solute carrier family 38, member 5	17	0.00	0.33	-4.15	-2.74	-4.75	-2.64	-3.75	-4.00
1372523_at	GCLC	glutamate-cysteine ligase, catalytic subunit	16	0.00	-0.32	-4.24	-3.72	-5.33	-3.70	-4.59	-3.29
1373458_at	BEX4	brain expressed, X-linked 4	9	0.00	0.33	-4.24	-26.55	-25.17	-23.87	-26.68	-5.09
1392687_at	PIGQ	phosphatidylinositol glycan anchor biosynthesis, class Q	16	-0.50	0.33	-4.30	-3.53	-6.43	-4.82	-3.90	-3.85
1372086_at	FHDC1	FH2 domain containing 1	17	-0.50	-0.33	-4.31	-1.95	-3.54	-3.33	-1.94	-4.49
1388059_a_at	SLC11A2	solute carrier family 11 (proton-coupled divalent metal ion transporters), member 2	16	0.00	-0.33	-4.37	-4.18	-4.55	-4.26	-4.36	-4.04
1369305_at	RAB3IL1	RAB3A interacting protein (rabin3)-like 1	17	0.00	-0.33	-4.40	-2.89	-3.91	-3.55	-2.69	-3.49
1367689_a_at	CD36	CD36 molecule (thrombospondin receptor)	15	0.00	0.33	-4.43	-1.92	-4.20	-3.22	-1.65	-3.95
1389507_at	NEDD4L	neural precursor cell expressed, developmentally down-regulated 4-like, E3 ubiquitin protein ligase	17	0.00	0.33	-4.49	-2.66	-5.11	-4.27	-2.69	-4.30
1387693_a_at	SLC6A9	solute carrier family 6 (neurotransmitter transporter, glycine), member 9	17	0.00	0.32	-4.50	-2.88	-4.21	-3.84	-2.98	-4.19
1393142_at	CEP70	centrosomal protein 70kDa	16	0.00	0.33	-4.59	-3.07	-5.11	-4.14	-3.79	-3.79
1395610_at	TSPAN33	tetraspanin 33	17	-0.49	-0.33	-4.62	-2.70	-4.79	-3.91	-3.61	-4.41
1375896_at	STRADB	STE20-related kinase adaptor beta	17	0.00	0.33	-4.65	-2.49	-4.43	-4.24	-2.62	-4.00
1392695_a_at	UROS	uroporphyrinogen III synthase	16	-0.50	0.33	-4.77	-6.07	-6.88	-6.03	-6.40	-5.84
1372374_at	CA1	carbonic anhydrase I	9	0.00	0.33	-4.78	-46.26	-64.49	-67.60	-43.94	-7.59
1387370_at	TMOD1	tropomodulin 1	17	0.00	0.33	-6.81	-3.78	-7.02	-5.18	-4.02	-7.72
1382618_at	EPB42	erythrocyte membrane protein band 4.2	17	-0.50	-0.33	-6.84	-3.25	-7.25	-5.11	-3.34	-8.67
1393376_at	SOX6	SRY (sex determining region Y)-box 6	17	0.01	0.31	-6.96	-4.84	-7.27	-6.53	-5.92	-6.58
1383853_at	DYRK3	dual-specificity tyrosine-(Y)-phosphorylation regulated kinase 3	17	0.00	0.33	-7.14	-2.62	-6.69	-6.60	-2.61	-8.69
1378196_at	SLC43A1	solute carrier family 43, member 1	17	0.00	-0.33	-7.70	-4.55	-10.31	-9.27	-5.39	-8.31
1369634_at	SLC4A1	solute carrier family 4	17	0.50	0.33	-7.89	-2.32	-5.68	-3.85	-2.15	-8.21
1371113_a_at	TFRC	transferrin receptor (p90, CD71)	15	0.00	-0.33	-8.14	-4.93	-15.11	-12.20	-4.97	-10.76
1389398_at	ANK1	ankyrin 1, erythrocytic	17	0.00	-0.33	-9.38	-4.35	-12.60	-7.48	-4.21	-12.30
1383290_at	SPINT1	serine peptidase inhibitor, Kunitz type 1	16	-0.50	-0.33	-9.60	-10.69	-13.97	-12.59	-11.11	-10.53
1388998_at	EPB49	erythrocyte membrane protein band 4.9 (dematin)	17	-0.50	0.33	-10.59	-5.70	-9.84	-8.05	-5.93	-10.33
1381477_at	ANK1	ankyrin 1, erythrocytic	17	0.00	0.33	-12.66	-6.64	-17.83	-10.27	-7.94	-14.31
1383286_at	PLEK2	pleckstrin 2	17	0.00	0.33	-14.00	-6.67	-15.65	-11.86	-9.34	-15.86
1387522_at	RHAG	Rh-associated glycoprotein	17	0.00	0.33	-14.97	-5.69	-13.90	-12.95	-6.28	-13.77
1381489_at			17	0.50	0.33	-17.14	-7.25	-22.67	-17.70	-9.82	-16.57
1387100_at	AQP3	aquaporin 3 (Gill blood group)	16	0.00	-0.33	-17.21	-8.44	-21.00	-13.40	-11.88	-12.18
138715_at	YPEL4	yippee-like 4 (Drosophila)	17	0.00	0.32	-19.98	-6.29	-15.03	-13.24	-7.82	-16.63
1386212_at	SPTA1	spectrin, alpha, erythrocytic 1 (elliptocytosis 2)	17	0.00	-0.33	-26.51	-4.34	-21.38	-11.00	-6.03	-29.53

Figures Legends

Figure 1. **Representative images of bone marrow hypocellularity in femur from male rats 24 hours after a single 30-minute IV infusion dose of oxaliplatin, topotecan or combination of oxaliplatin followed by topotecan.** Hematoxylin and eosin stained tissue sections; 10X objective; bars = 100 μ m. (A) Male rat exposed to vehicle control. (B) Minimal hypocellularity in male rat exposed to oxaliplatin. (C) Mild hypocellularity in male rat exposed to topotecan. (D) Moderate hypocellularity in male rat exposed to oxaliplatin followed by topotecan. Bone marrow hypocellularity was graded based on the estimated percentage of cell loss with minimal hypocellularity = 10 to 20% cell loss, mild hypocellularity = 30 to 40% cell loss, moderate hypocellularity = 50 to 60% cell loss, and marked hypocellularity = greater than 60% cell loss.

Figure 2. **EPIG patterns across treatments groups 1, 6, and 24-hours post treatment.** The average of the \log_2 ratio (treated sample to the average of the time-matched control) from the top 6 expression profiles with the highest degree of correlation are plotted and displayed on the y-axis. The x-axis contains the treatments and the order of exposure. Ox = oxaliplatin (15 mg/kg) and To = topotecan (4.7 mg/kg). **A.** Patterns extracted by EPIG of mRNA from bone marrow samples that were collected one-hour post treatment administration. The row labeled 1st denotes which agent was administered first. **B.** Same as A except analysis of mRNA from bone marrow samples that were collected **6 hours post treatment**. **C.** Same as A except analysis of mRNA from bone marrow samples collected **24 hours post treatment**.

Figure 3. **Heatmap of gene expression data analyzed by EPIG.** A) The 1393 gene probes categorized to the 16 EPIG patterns (y-axis color column) across the 1, 6 and 24 hour time points are in rows and the samples are in columns. B) Patterns 8, 9, 11, 14 – 16 from the samples at just the 1-hour time point. The

labeling of samples is according to the time and order in which the agent was given (either 1st or second). Ox is oxaliplatin (15 mg/kg) and To = topotecan (4.7 mg/kg). Veh1 is the vehicle used for Ox, and Veh2 is the vehicle used for To. The data is the \log_2 ratio (treated sample to the average of the time-matched control) and the scale on the bottom displays the color range for the \log_2 ratio values. Red denotes upregulation, blue downregulation, and grey relatively no change.

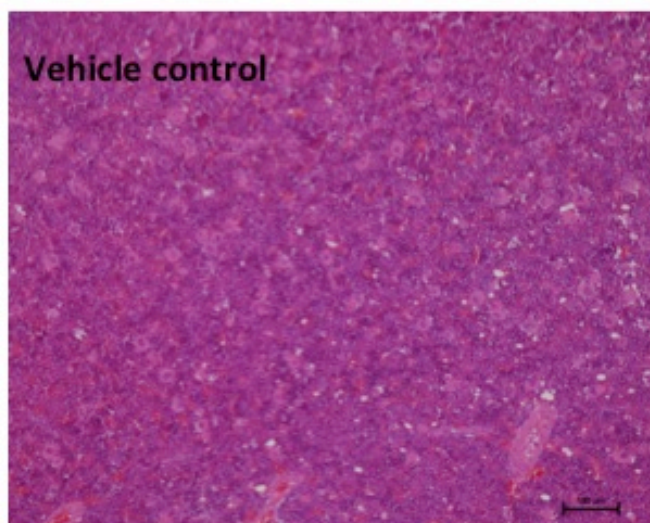
Figure 4. Scatter plots of pathways enriched in patterns derived from bone marrow collected post-treatment with topotecan, oxaliplatin, or a combination. Clusters of genes identified by EPIG were then analyzed using Gene Set Enrichment Analysis (GSEA) and Sub-Network Enrichment Analysis (SNEA) algorithms to find enriched pathways. **A.** One hour post treatment **B.** Six hours post treatment **C.** Twenty-four hours post treatment. Treatments were oxaliplatin (Ox; 15 mg/kg) and topotecan (To; 4.7 mg/kg). Veh1 is the vehicle used for oxaliplatin, and Veh2 is the vehicle used for topotecan. The numbers on the x-axis denote the EPIG pattern which contained the genes that enriched the pathways labeled on the y-axis. A square represents a pathway that was enriched by the genes in the given EPIG pattern.

Figure 5. Clustering of the Enrichment of GO BPs. Clustering and heatmap based on the $-\log_{10}(p\text{-values})$ of the 641 Gene Ontology (GO) biological processes (BPs) for each treatment and time point. The GO BPs are on the y-axis, the samples are on the x-axis. The enriched GO BPs were obtained from limma analysis DEGs (absolute fold change > 2 and FDR < 0.01). Significance of enrichment was set to $p\text{-value} < 0.05$. Missing values were imputed as 0 ($-\log_{10}(1)$, i.e. $p\text{-value}=1$). Clustering of the pathways were performed using Pearson correlation dissimilarity (r) and average linkage grouping. Clusters (those with a $1-r$ value ≥ 0.9) of GO BP terms ($n \geq 30$) were labeled according to the node having the maximum number of paths to it within the GO BP subtree directed acyclic graph derived from the terms in the cluster. The color in the legend denotes the significance of enrichment. The more red the heat map color, the more significant the enrichment.

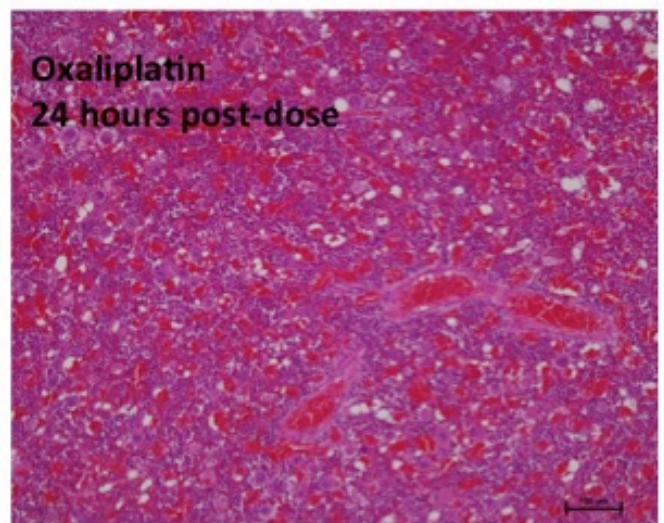
Figure 6. **Overlay of gene expression on the p53 signaling pathway.** The rat p53 signaling pathway is overlaid with the average of the log base 2 ratio values from the replicate samples. Red denotes induction, green repression. Grey indicates that the gene was not mapped. The legend illustrates the segmentation of the genes according to the data from a given treatment.

Figure 7. **Reconstruction of the p53 signaling gene regulatory network.** The 19 genes mapped in the rat p53 signaling Wikipathway is used to reconstruct the network based interactions derived from the gene expression data. For (A) topotecan followed by oxaliplatin and (B) oxaliplatin followed by topotecan, the average of the biological replicates' gene expression data at each time point were used to reconstruct the gene regulatory network depending of the order of administration of the two drugs. A red arrow indicates activation, a blue arrow indicates inactivation. The labeling of the nodes is based on the UniGene symbol.

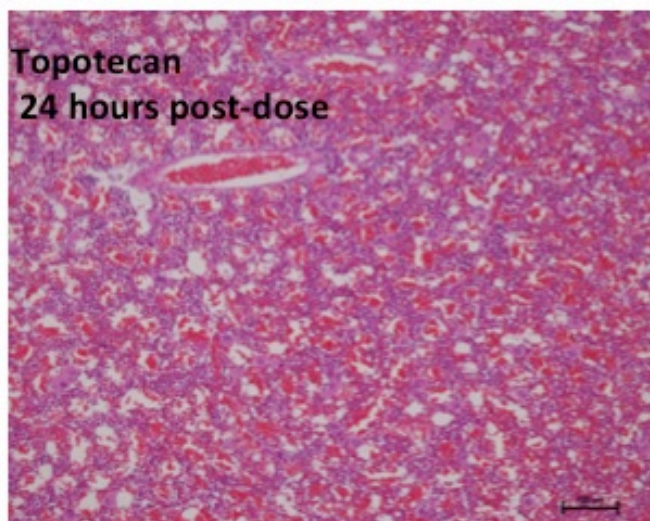
Figure 1.JPEG



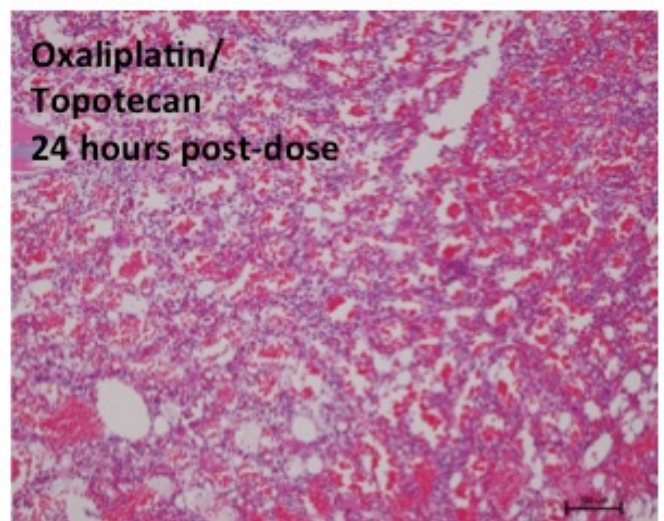
Normal – no lesions



Minimal hypocellularity



Mild hypocellularity



Moderate hypocellularity

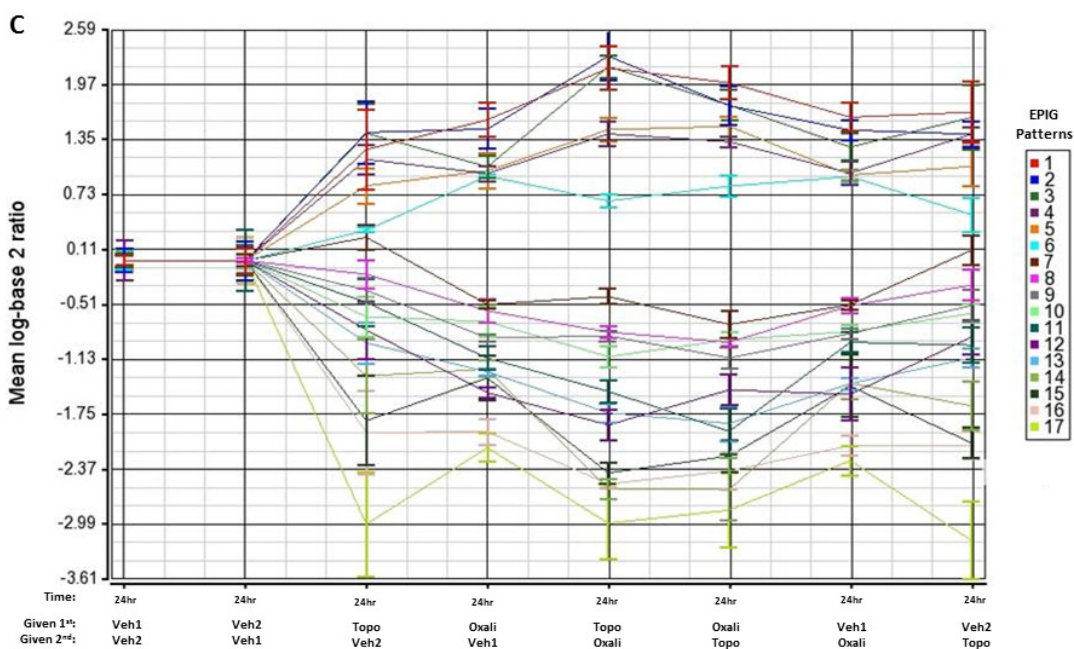
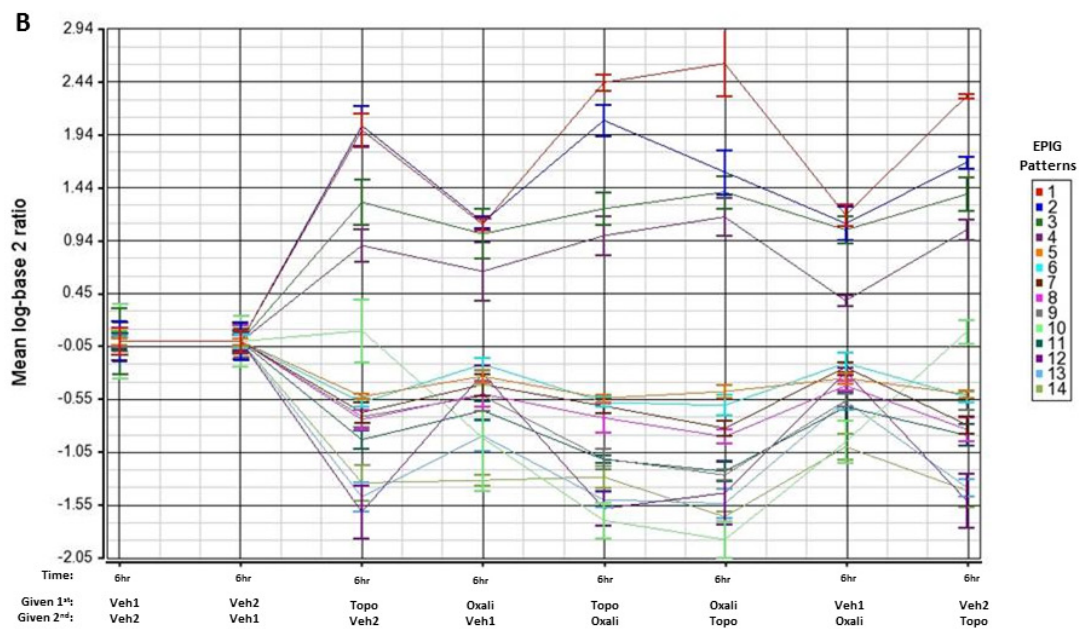
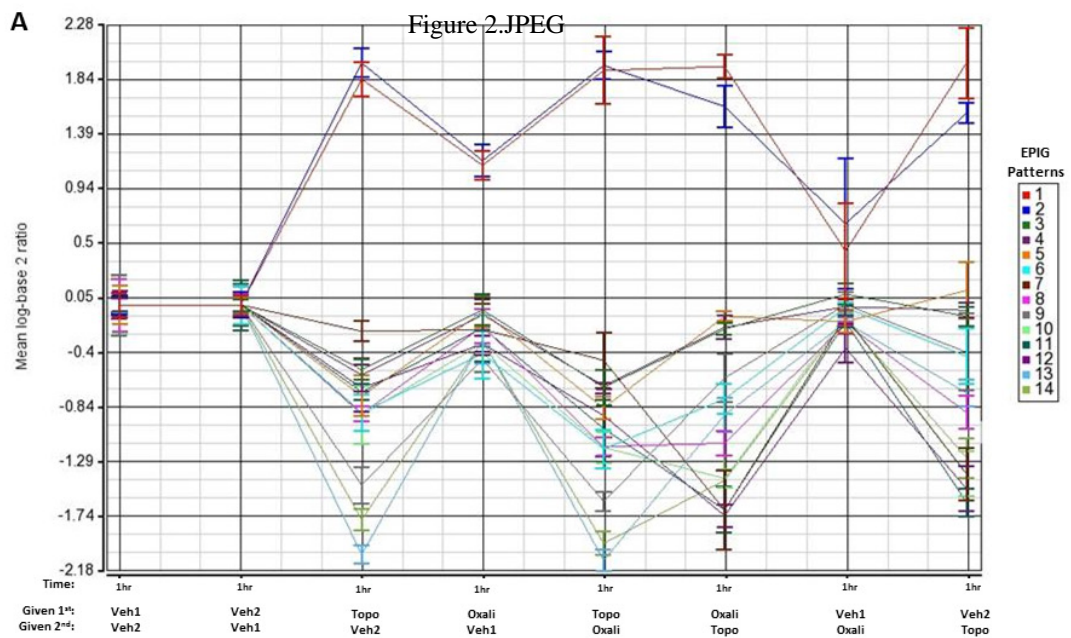
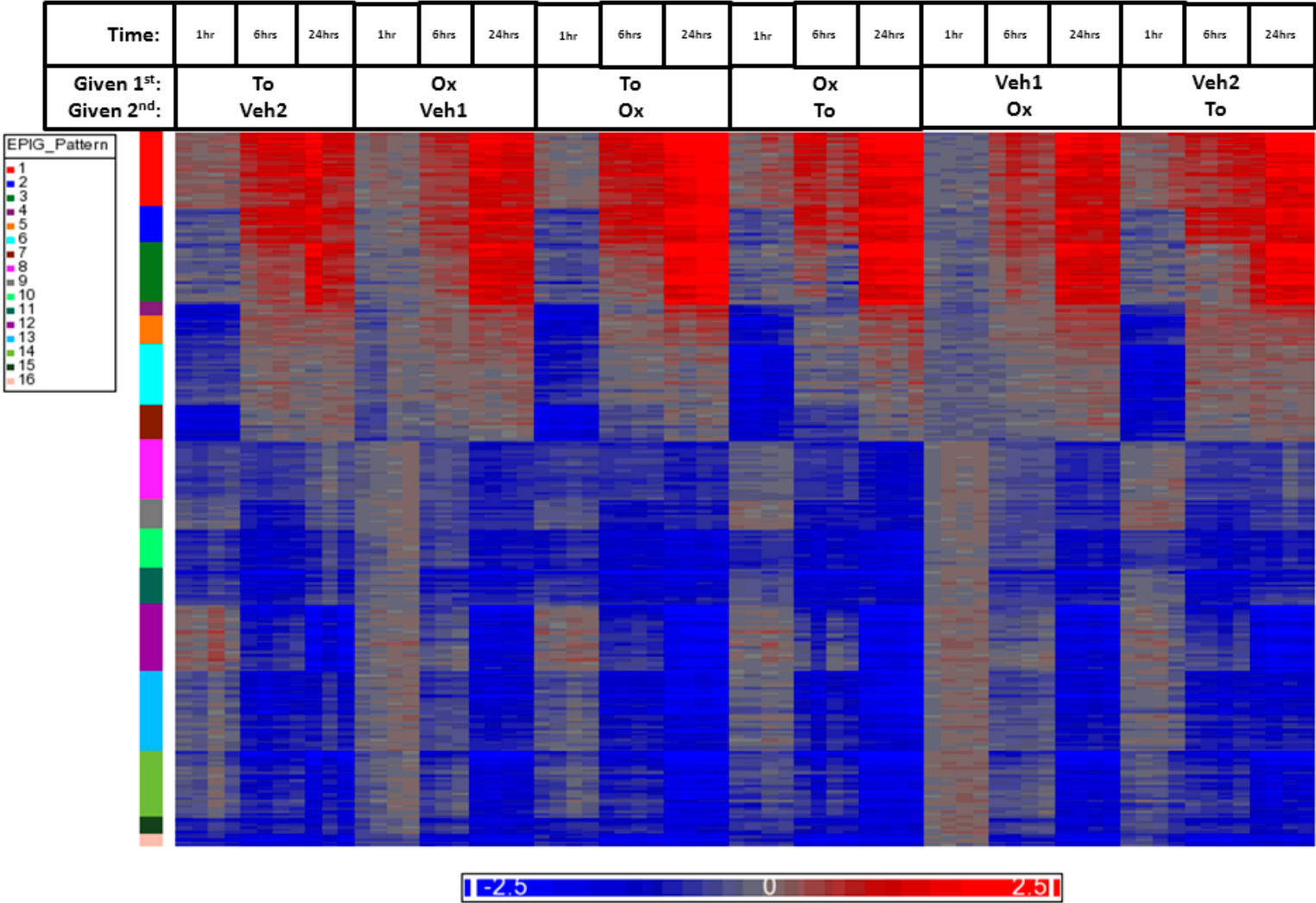
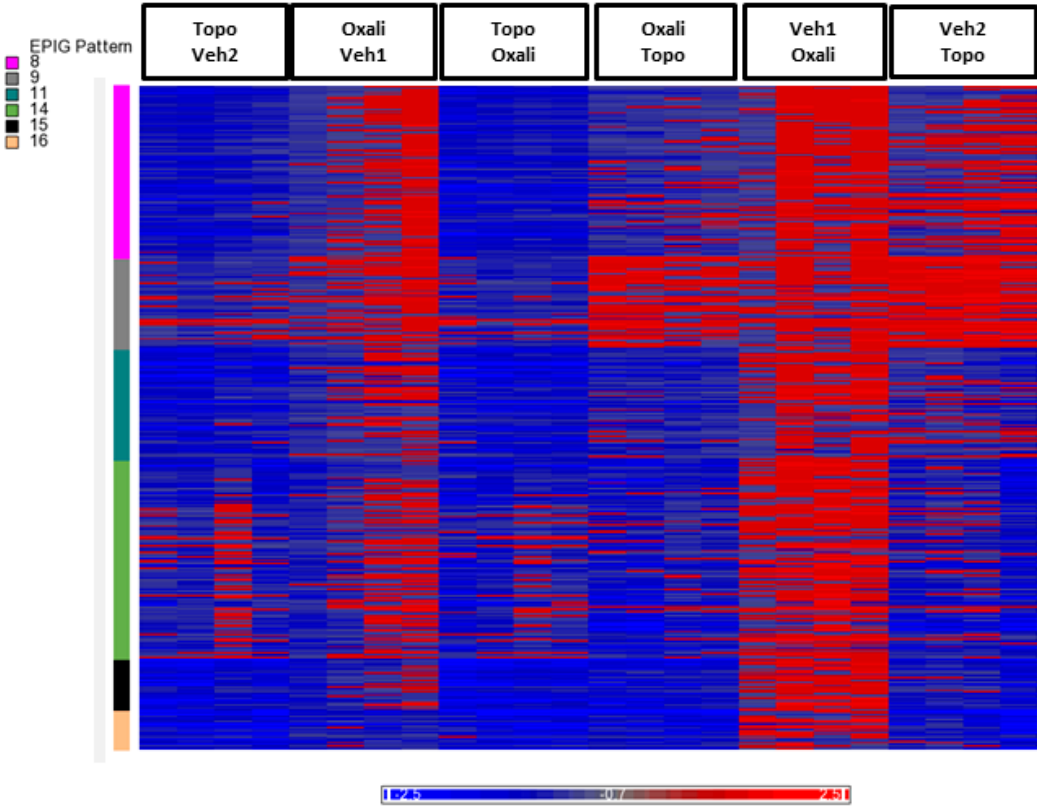


Figure 3.TIF

(A)



(B)



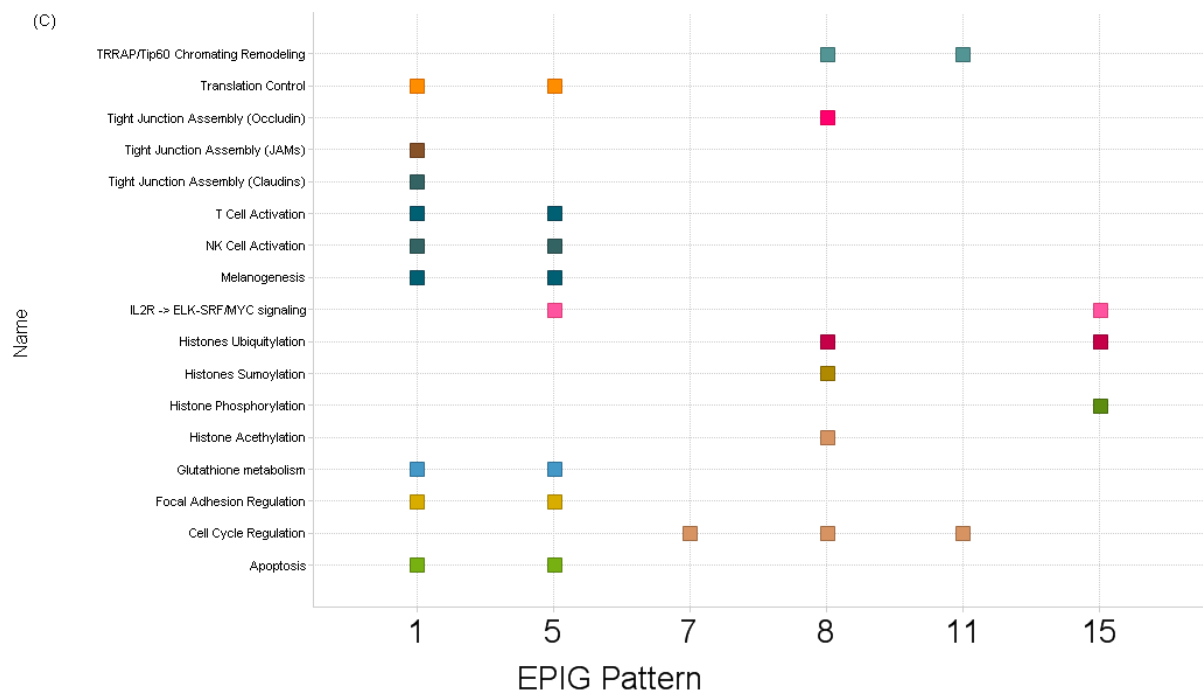
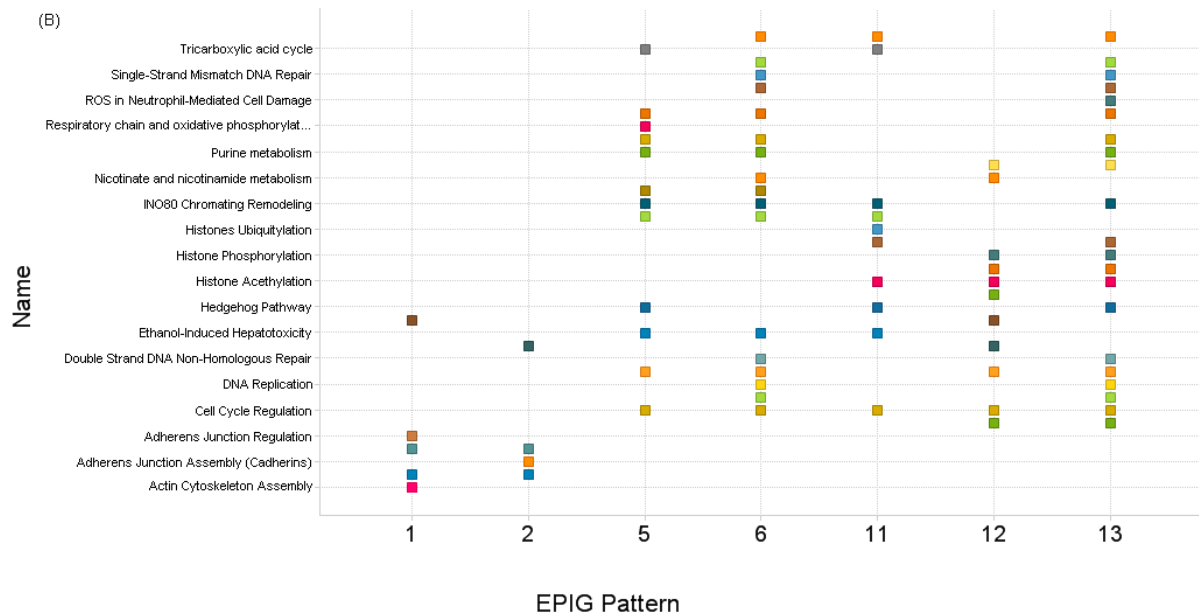
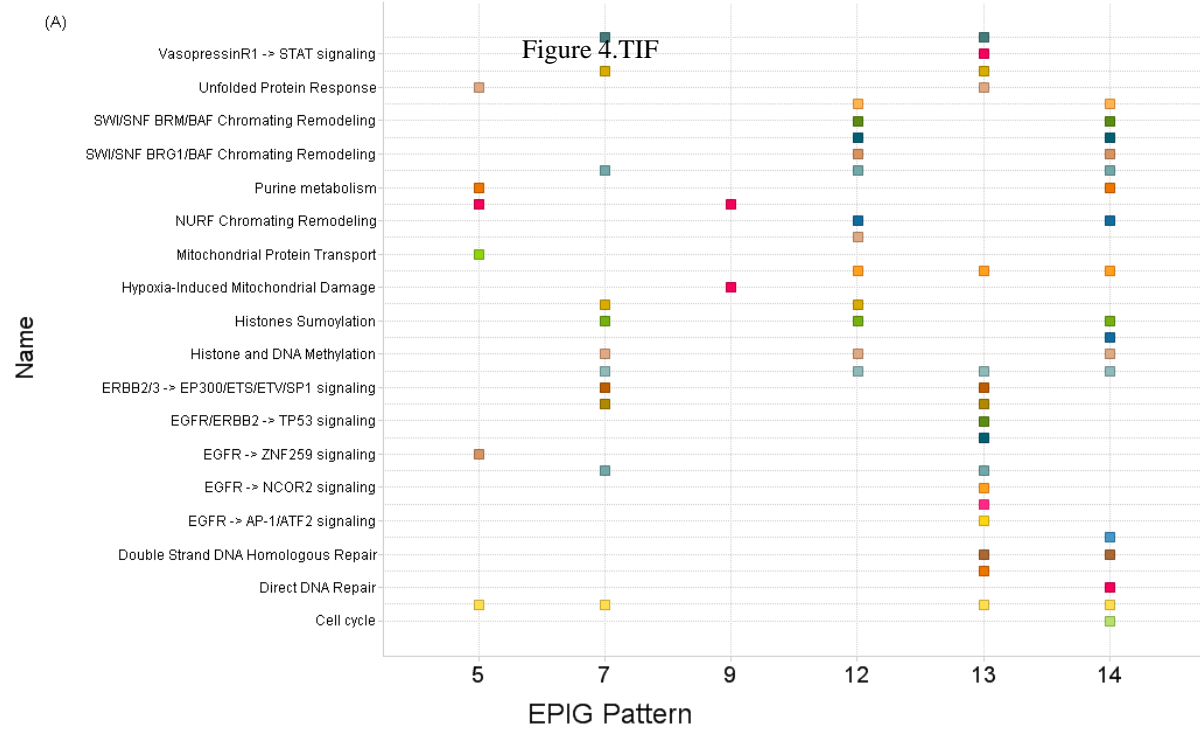


Figure 5.TIF

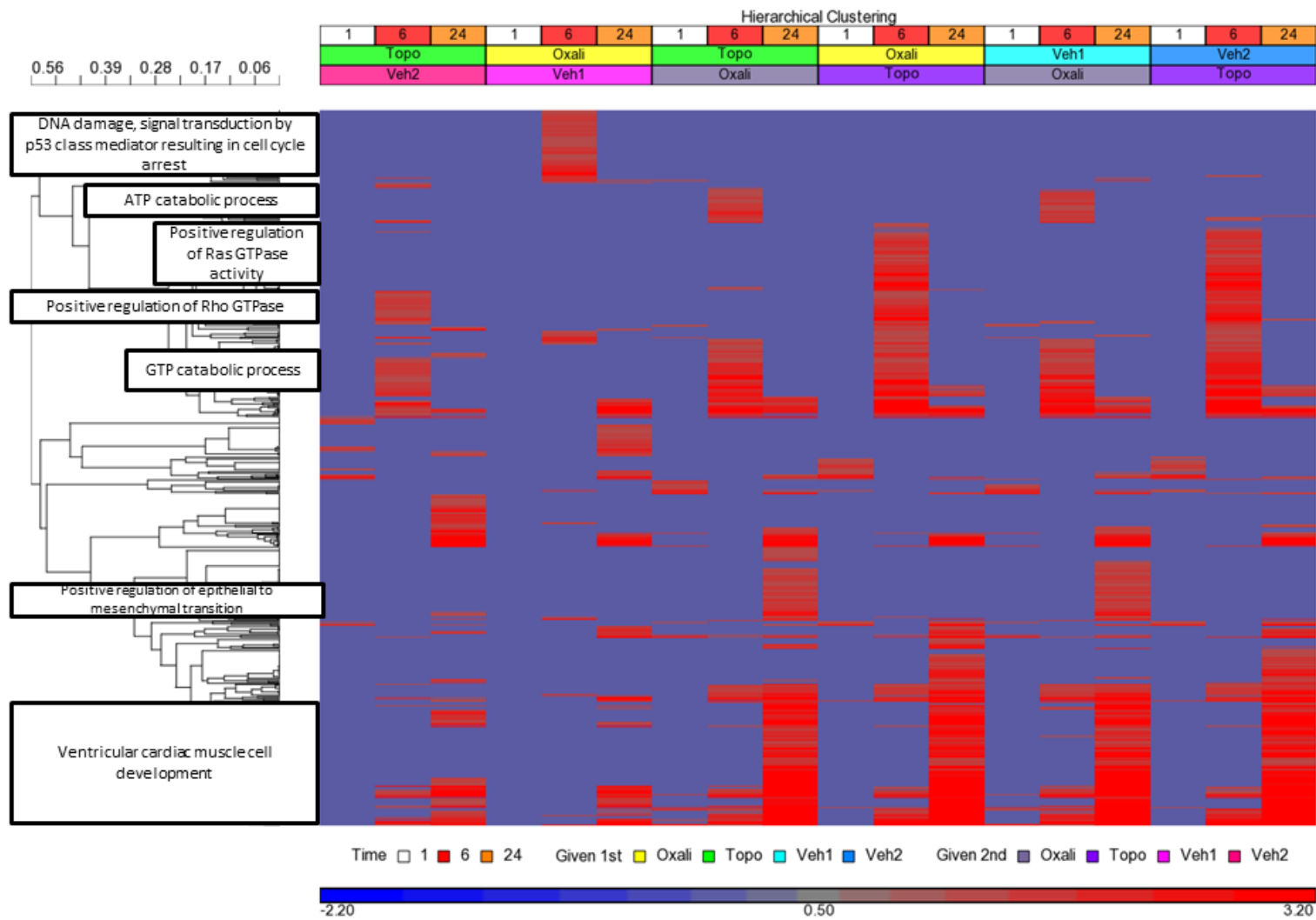
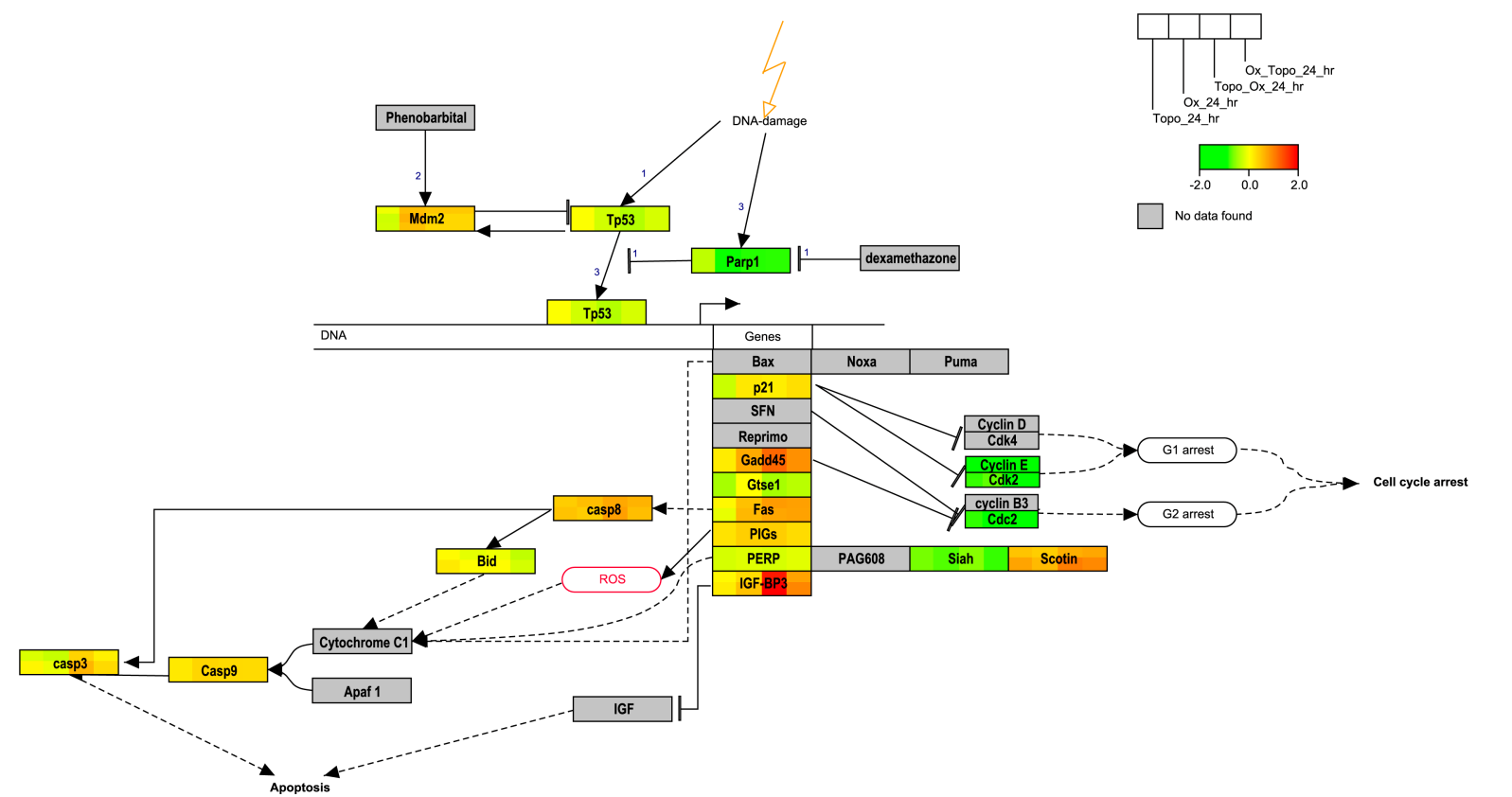
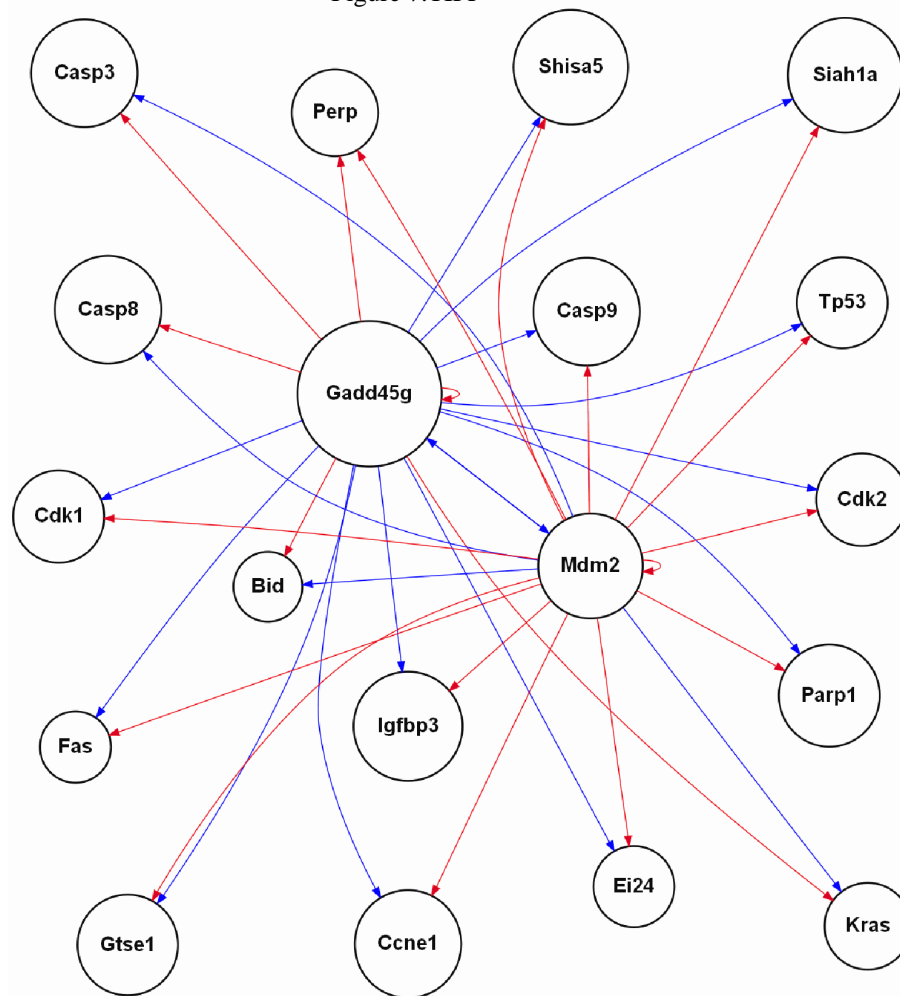


Figure 6.TIF



(A)

Figure 7.TIFF



(B)

